Title
Regulation of translation and mRNA stability in early mammalian development

Permalink
https://escholarship.org/uc/item/1rq6w1bf

Author
Freimer, Jacob W

Publication Date
2018

Peer reviewed|Thesis/dissertation

Regulation of translation and mRNA stability in early mammalian
development

by

Jacob Freimer

DISSERTATION

Submitted in partial satisfaction of the requirements for the degree of

DOCTOR OF PHILOSOPHY

in

Developmental and Stem Cell Biology

in the

GRADUATE DIVISION

of the

UNIVERSITY OF CALIFORNIA, SAN FRANCISCO

Approved:

For my parents, Sally and Nelson

<u>Acknowledgements</u>

Finally, I am grateful for my wonderful family. I would like to thank my parents and my brother for all of their love and support. I could not have asked for better role models, as parents and as scientists, than my mom and dad. They have always encouraged and supported my curiosity and goals from taking apart the radio when I was 2 years old to pursuing a Ph.D. Lastly, I would like to thank my significant other Amanda for her constant love, encouragement, and positivity.

Contributions

The research presented in this thesis was conducted under the supervision of Dr. Robert Blelloch at the University of California, San Francisco. This work was supported by a Genentech predoctoral fellowship.

Chapter 2 describes work published in *Current Biology* in 2018 with the following authors: Jacob Freimer, Raga Krishnakumar, Matthew Cook, and Robert Blelloch. Raga Krishnakumar performed all of the Xenopus experiments. Matthew Cook performed the initial mouse experiments. I performed the additional mouse experiments including all of the transgenic experiments, the RNA-Seq, and the microarrays. Raga Krishnakumar and I jointly analyzed the data. Robert Blelloch supervised the research. Raga Krishnakumar, Robert Blelloch, and I wrote the manuscript.

Chapter 3 describes work in preparation for submission to *eLife* with the following authors: Jacob Freimer, TJ Hu, and Robert Blelloch. TJ Hu assisted with the western blots and the polysome profiling experiments. I performed all of the other experiments and analyzed the data under the supervision of Robert Blelloch. Robert Blelloch and I wrote the manuscript. All of the writing in this thesis is my own.

Regulation of translation and mRNA stability in early mammalian development
Jacob Freimer

Abstract

Post-transcriptional regulation is critical to ensure precise control of mRNA and protein levels. Here we characterize the regulation of mRNA stability and translation, focusing on the impact of microRNAs, in two systems in early mouse development.

Mouse oocyte maturation, fertilization, and reprogramming occur in the absence of transcription and thus changes in mRNA levels and translation rate are regulated through post-transcriptional mechanisms. Surprisingly, microRNA function is absent during this critical period of mammalian development. In Chapter 2 we investigated the mechanisms underlying the global suppression of microRNA activity. In both mouse and frogs, microRNA function was active in growing oocytes, but then absent during oocyte maturation. RNA-Seq of mouse oocytes uncovered that the microRNA effector protein AGO2 is predominantly expressed as an alternative isoform that encodes a truncated protein lacking all of the known essential domains. Full length *Ago2* as well as the related Argonautes (*Ago1*, *Ago3*, and *Ago4*) were lowly expressed in maturing mouse oocytes. Reintroduction of full-length AGO2 together with an exogenous microRNA in either mouse or frog oocytes restored translational repression of a target reporter. However, levels of endogenous transcripts remained unchanged. Consistent with a lack of microRNA activity, analysis of transcripts with alternative polyadenylation sites showed increased stability of transcripts with a longer 3' UTR during oocyte maturation. Redundant mechanisms protecting endogenous transcripts and the conserved loss of microRNA activity suggest a strong selection for suppressing microRNA function in vertebrate oocytes.

Translation and mRNA degradation are intimately connected, yet the mechanisms that regulate both are not fully understood. In Chapter 3, we examine the regulation of translation and mRNA stability in mouse embryonic stem cells (ESCs) and during differentiation. In contrast to previous reports, we found that transcriptional changes account for most of the molecular changes during ESC differentiation. However, within ESCs there was a positive correlation between translation level and mRNA stability. We asked if the RNA-binding protein DDX6 links these processes in ESCs since the yeast homolog of DDX6 connects codon optimality and mRNA stability. However, there was minimal connection between codon usage and stability changes in DDX6 KO ESCs. DDX6 has also been implicated in microRNA mediated repression, a process involving both translational repression and mRNA destabilization. Surprisingly, the loss of DDX6 leads to the translational derepression of microRNA targets without affecting mRNA stability. Furthermore, DDX6 KO ESCs share overlapping phenotypes and global molecular changes with ESCs that completely lack all microRNAs. Together our results demonstrate that it is possible to decouple the two forms of microRNA induced repression and emphasize that the translational aspect of microRNA repression is underappreciated.

Together these studies provide new insights into how microRNA activity is regulated as well as the downstream effectors that carry out microRNA induced translational repression.

Table of Contents

List of Figures

Chapter 1 - Introduction

Early mammalian development

The transition from an oocyte to a totipotent zygote is one of the most dynamic cell fate transitions in mammalian development. During this transition, the oocyte matures, completes meiosis, becomes fertilized, and the resulting zygote then undergoes a dramatic epigenetic reprogramming (Saitou et al. 2012; Cantone & Fisher 2013). The zygote then undergoes a number of cleavage divisions and the first specification events (reviewed in (Kojima et al. 2014)). By embryonic day 3.5, the embryo has formed a blastocyst composed of a cluster of cells called the inner cell mass and extraembryonic trophectoderm that will give rise to the embryo proper and placenta respectively. The cells in the epiblast are considered pluripotent because they are capable of giving rise to every tissue in the adult organism. At embryonic day 6.5, the pluripotent cells of the embryo proper become further specialized as they differentiate into the three germ layers: mesoderm, endoderm, and ectoderm during a process called gastrulation.

Mouse embryonic stem cells (ESCs) represent an ideal model to study the regulation of early development, enabling mechanistic studies that are difficult to perform in vivo. ESCs can be cultured in a self-renewing, pluripotent state in the presence of leukemia inhibitory factor (LIF) (Nichols & Smith 2010). Further refinement of culture conditions showed that the addition of a MEK inhibitor and a GSK3b inhibitor (2i) maintain ESCs in a more homogenous state termed naive pluripotency that closely resembles the peri-implantation embryo at embryonic day 4.5 (Boroviak et al. 2015; Ying et al. 2008). The isolation of ESCs has enabled extensive characterization of the signaling, transcriptional, epigenetic, and post-transcriptional programs that regulate both pluripotency and early development (Young 2011; Watanabe et al. 2013; Ng & Azim Surani 2011; Ye & Blelloch 2014; Chen & Hu 2017). Furthermore, ESCs have enabled

the creation of knockout mice, transforming the ability to characterize the function of individual genes in mammals (Guan et al. 2010). It is also possible to coax ESCs to differentiate into a myriad of cell types *in vitro* further enabling mechanistic studies of many different adult stem cell populations and mature cell types (Murry & Keller 2008).

The early stages of embryonic development must be tightly regulated to ensure that the small number of cells in the early embryo faithfully give rise to every tissue in the adult organism. Remarkably, oocyte maturation and fertilization occur in the absence of RNA Polymerase II-directed transcription and thus any changes in mRNA must occur post-transcriptionally (Abe et al. 2010). This regulation is especially critical since, in the absence of transcription, there is no mechanism to replace degraded mRNAs. In mammals, oocytes are set aside early and then held in a dormancy in some cases for many years prior to fertilization (Lei & Spradling 2013). Therefore, any regulatory mechanism affecting the level of RNA has to be tightly controlled. In ESCs, it has been proposed that post-transcriptional regulation accounts for up to 70% of the molecular changes during ESC differentiation (Lu et al. 2009). Furthermore, several hundred RNA-binding proteins are preferentially expressed in the ESC state and many RNA-binding proteins are specifically up-regulated during induced pluripotent stem cell reprogramming suggesting that post-transcriptional regulation plays a vital role in ESC biology (Kwon et al. 2013). Additionally, microRNAs, another key post-transcriptional regulator, play key roles in regulating ESC self-renewal and differentiation (Melton et al. 2010). Despite the evidence that post-transcriptional regulation is critical during early mammalian development, many questions remain about the specific regulatory mechanisms in both oocytes and ESCs.

microRNAs in early mammalian development

Small non-coding RNAs are important post-transcriptional regulators. In mammals, microRNAs (miRNAs) are the major class of small non-coding RNAs in most tissues (Chiang et al. 2010; Babiarz et al. 2008). MiRNAs are initially transcribed as primary miRNAs, which are long single-stranded RNAs that contain one or several stem loops (Krol et al. 2010). The microprocessor complex consisting of DROSHA and DGCR8 cleaves the stem loop of primary miRNAs to generate precursor miRNAs (Krol et al. 2010). EXPORTIN-5 exports precursor miRNAs from the nucleus to the cytoplasm where they are cleaved by the enzyme DICER to generate ~ 22 nucleotide mature miRNAs (Krol et al. 2010). Mature miRNAs are loaded into one of four Argonaute proteins (AGO1-4) to form the RNA-induced silencing complex (RISC) (Fabian & Sonenberg 2012; Bartel 2009). The miRNA-RISC typically binds to the 3' UTR of hundreds of target mRNAs (Fabian & Sonenberg 2012; Bartel 2009). If the miRNA is loaded in AGO2 and perfectly complements the target 3' UTR, it is capable of endonucleolytic cleavage (Liu et al. 2004). However, miRNAs typically bind through partial complementary binding; target specificity is primarily governed by complementarity between nucleotides 2-7 of the miRNA (called the seed sequence) and the target's 3' UTR. In this case, miRNA-RISC interacts with a number of proteins to inhibition translation and/or induce mRNA degradation of target transcripts (Jonas & Izaurralde 2015). miRNA repression often leads to the removal of the 5' cap, deadenylation of the poly(A) tail, and eventual exonucleolytic degradation by XRN1 of the target mRNA (Jonas & Izaurralde 2015). However, whether miRNAs primarily inhibit translation or induce mRNA destabilization is still debated.

The development of knockout models of DGCR8, DROSHA, DICER, and AGO2 has enabled the dissection of miRNA function in different tissues including oocytes and early embryos (Bernstein et al. 2003; Morita et al. 2007; Chong et al. 2010; Wang et al. 2007). Surprisingly, DGCR8 knockout oocytes show no gene expression changes, mature normally,

can be fertilized, and produce healthy pups (Suh et al. 2010). Additionally, reporter studies in

oocytes show a lack of miRNA induced repression (Ma et al. 2010). These results suggest that

miRNAs play no role in mouse oocytes. In contrast, constitutive knockouts for DGCR8,

DROSHA, DICER, and AGO2 are embryonic lethal and conditional knockouts lead to severe

phenotypes of the targeted tissue (Shenoy & Blelloch 2014). Furthermore, deletion of DGCR8,

DICER, or AGO2 in ESCs result in severe proliferation and differentiation defects.

Multiple miRNAs that share similar seed sequences are grouped into a miRNA family

(Friedman et al. 2008). Since miRNA family members share similar seed sequences, they are

thought to bind to overlapping sets of targets. In early embryos and ESCs the embryonic stem

cell enriched cell cycle (ESCC) family is the dominant miRNA family (Greve et al. 2013;

Houbaviy et al. 2003; Marson et al. 2008). This family is composed of two clusters of miRNAs,

the miR-290~295 cluster and the miR-302~367, which are expressed sequentially in early

mouse development (Parchem et al. 2014). These miRNAs are vital for promoting the unique

cell cycle of ESCs, play key roles in promoting self-renewal, and strongly enhance the

reprogramming of somatic cells to pluripotent cells (Subramanyam et al. 2011; Melton et al.

2010; Wang et al. 2008).

Regulation of translation and RNA stability

The translation of mRNA into proteins is a complex, highly regulated process (reviewed

in (Sonenberg & Hinnebusch 2009; Jackson et al. 2010; Hinnebusch 2014). Translation occurs

in several stages: initiation, elongation, termination, and ribosome recycling. The majority of

translational regulation is thought to occur through control of the initiation phase. Translation

initiation begins by the eIF4F complex binding to the 5' cap of the mRNA. The eIF4F complex

consists of eIF4E, eIF4A, and eIF4G; eIF4E directly binds to the 5' cap, eIF4A is a DEAD box

RNA helicase that helps unwind the RNA to allow the 43S preinitiation complex to bind and begin scanning the RNA, and eIF4G is a large scaffold protein that interacts with other proteins to facilitate and enhance translation initiation (Sonenberg & Hinnebusch 2009). Separately, eIF3, eIF1, eIF1A, and the ternary complex (eIF2-methionyl-tRNAi-GTP) bind to the 40S ribosomal subunit to form the 43S preinitiation complex (Hinnebusch 2014). eIF3 interacts with the eIF4G scaffold to bring the 43S preinitiation complex to the mRNA, where it can begin scanning the 5' UTR. The 43S complex scans through the 5' UTR until it locates an AUG start codon in a suitable context to begin translation. Recognition of the start codon leads to the hydrolysis of eIF2-GTP to eIF2-GDP followed by the release of eIF2 and several other eIFs (Hinnebusch 2014). The release of these factors enables the 60S ribosomal subunit to bind the 43S subunit catalyzed by eIF5B (Hinnebusch & Lorsch 2012). Binding of the 60S subunit with the 43S subunit forms a complete 80S ribosome allowing translational elongation to proceed. Additionally, the poly(A) binding protein, PABP, interacts with eIF4G and the poly(A) tail of the mRNA. This interaction is thought to link the 5' cap with the poly(A) tail in a closed loop confirmation that enhances translation initiation and promotes efficient reinitiation after the ribosome finishes translation (Jackson et al. 2010; Hinnebusch 2014). However, a recent paper challenges the idea that the majority of translation occurs in a closed loop (Adivarahan et al. 2017). Future studies will likely resolve whether the closed loop structure is transcript, context, or cell type dependent in mammalian cells.

Translation is regulated by both RNA-binding proteins and miRNAs. RNA-binding proteins can modulate the binding of translation initiation factors, modulate RNA structure, and directly affect ribosome movement (reviewed in (Ye & Blelloch 2014; Szostak & Gebauer 2013). One particularly interesting translational repressor is the DEAD box helicase protein DDX6 and its yeast homolog DHH1 (Presnyak & Coller 2013). The loss of DHH1 leads to translational

derepression, disrupted P-body formation, and the stabilization of mRNAs (Coller & Parker 2005). Tethering experiments in yeast with decapping or exonuclease mutants suggest that DHH1 can repress translation independent of enhancing decapping (Sweet et al. 2012; Carroll et al. 2011). In human cells, direct tethering of DDX6 also represses translation (Kuzuoğlu-Öztürk et al. 2016). How DDX6 represses translation is not fully understood. However, it was recently shown that DDX6 interacts with 4E-T, which competes with eIF4G for binding to the translation initiation factor eIF4E and leads to translational repression (Kamenska et al. 2016; Ozgur et al. 2015). DDX6 also binds to components of the decapping complex, potentially enhancing the removal of the 5' cap and leading to reduced translation (Ayache et al. 2015; Tritschler et al. 2009; Nissan et al. 2010). Additionally, through interactions with the CCR4-NOT complex and the decapping complex, DDX6 is involved in miRNA mediated translational repression, but its exact role is not fully understood (Chen et al. 2014; Mathys et al. 2014; Rouya et al. 2014; Chu & Rana 2006).

In addition to promoting translation, the 5' cap and poly(A) tail stabilize the mRNA and prevent non-specific degradation. Recent high-throughput measurements have estimated that the median mammalian poly(A) length is between 50-100 nucleotides (Subtelny et al. 2014; Chang et al. 2014). Deadenylation of the poly(A) tail by the CCR4-NOT and PAN2-PAN3 complexes is typically the initial and rate limiting step for RNA degradation (Wahle & Sebastiaan Winkler 2013). After deadenylation, DCP2 catalyzes hydrolysis of the 5' mRNA cap (Arribas-Layton et al. 2013). DCP1, EDC3, and EDC4 enhance the activity of DCP2 (Arribas-Layton et al. 2013). Following removal of the 5' cap, most mRNA is degraded by the 5' to 3' exonuclease XRN1 (Nagarajan et al. 2013). However, following removal of the poly(A) tail, RNA can also be degraded 3' to 5' by the exosome complex (Nagarajan et al. 2013). Mammalian mRNAs display a wide range of half-lives ranging from minutes to over a day

(Schwanhäusser et al. 2011). However, many of the upstream factors that control the frequency with which a transcript enters the degradation pathway are not well understood. Both RNA-binding proteins and miRNAs can alter the stability of their targets.

miRNAs can both repression translation and induce mRNA destabilization of their targets. Repression starts through miRNA-AGO complexes binding to their target transcripts. GW182 (TNRC6) then binds to AGO and recruits a number of additional proteins involved in translational repression and mRNA degradation. miRNAs are thought to inhibit translation initiation, but individual studies do not agree on the primary factors or mechanism that are targeted (Jonas & Izaurralde 2015). miRNAs might disrupt translation initiation by disrupting eIF4A binding and activity (Fukao et al. 2014; Fukaya et al. 2014). miRNAs have also been shown to recruit translational repressors such as DDX6 (Chen et al. 2014; Mathys et al. 2014; Rouya et al. 2014; Chu & Rana 2006). Recruitment of GW182 also leads to the displacement of PABP, potentially reducing translation and making the poly(A) tail accessible for deadenylation (Moretti et al. 2012; Zekri et al. 2013). MiRNAs promote mRNA degradation by recruiting the canonical degradation machinery. GW182 directly recruits the PAN2-PAN3 and CCR4-NOT deadenylation complexes (Chen et al. 2014; Mathys et al. 2014; Christie et al. 2013). Additionally, miRNA activity, partially through recruitment of DDX6, leads to recruitment of the decapping complex (Tritschler et al. 2009; Nishihara et al. 2013). Following decapping and deadenylation, miRNA targets get degraded by XRN1. Since miRNA activity leads to the removal of the 5' cap and the poly(A) tail, both of which reduce translation and mRNA stability, disentangling the primary mechanism of action has been complicated and controversial.

Translational repression vs mRNA destabilization of miRNA targets

Whether miRNAs primarily act through translation repression or mRNA degradation has been intensely debated (Jonas & Izaurralde 2015; Iwakawa & Tomari 2015). Ribosome profiling and RNA-seq experiments demonstrate that miRNAs typically both inhibit the translation of and destabilize their mRNA targets (Guo et al. 2010; Eichhorn et al. 2014). In both of these studies, the mRNA fold change is larger than the change in translational efficiency and the studies conclude that mRNA destabilization is the dominant effect. However, ribosome profiling and RNA-seq in the early zebrafish embryo found that miRNAs induce translational repression without mRNA destabilization (Bazzini et al. 2012). Furthermore, experiments using miRNA reporters to examine the kinetics of miRNA repression suggest that translational repression precedes mRNA destabilization (Djuranovic et al. 2012; Béthune et al. 2012). These studies pose the question of whether translation repression is the primary mode of suppression and that mRNA destabilization is a consequence of translation repression. Despite extensive research, it is not known whether it is possible to decouple translational repression and RNA destabilization in a cell where both occur. Additionally, it is unclear whether translational repression of miRNA targets is a prerequisite for their decay.

Premise of these studies

miRNAs are critical post-transcriptional regulators, yet many questions about how miRNA activity is regulated remain unanswered. In the following chapters, I present my contributions to the field. In chapter 2, I show that suppression of miRNA activity in oocytes occurs via redundant mechanisms--limiting levels of functional AGO/miRNA complexes together with AGO-independent protection of endogenous transcripts. In chapter 3, I show how the loss of the RNA-binding protein DDX6 decouples translational repression from mRNA destabilization of miRNA targets in mouse ESCs.

Chapter 2 - Expression of alternative Ago2 isoform associated with loss of microRNA driven translational repression in mouse oocytes

Summary

Mouse oocyte maturation, fertilization, and reprogramming occur in the absence of transcription and thus changes in mRNA levels and translation rate are regulated through post-transcriptional mechanisms (Abe et al. 2010). Surprisingly, microRNA function, which is a major form of post-transcriptional regulation, is absent during this critical period of mammalian development (Ma et al. 2010; Suh et al. 2010). Here, we investigated the mechanisms underlying the global suppression of microRNA activity. In both mouse and frogs, microRNA function was active in growing oocytes, but then absent during oocyte maturation. RNA-Seq of mouse oocytes uncovered that the microRNA effector protein AGO2 is predominantly expressed as an alternative isoform that encodes a truncated protein lacking all of the known essential domains. Full length *Ago2* as well as the related Argonautes (*Ago1*, *Ago3*, and *Ago4*) were lowly expressed in maturing mouse oocytes. Reintroduction of full-length AGO2 together with an exogenous microRNA in either mouse or frog oocytes restored translational repression of a target reporter. However, levels of endogenous transcripts remained unchanged. Consistent with a lack of microRNA activity, analysis of transcripts with alternative polyadenylation sites showed increased stability of transcripts with a longer 3' UTR during oocyte maturation. Redundant mechanisms protecting endogenous transcripts and the conserved loss of microRNA activity suggest a strong selection for suppressing microRNA function in vertebrate oocytes.

This study was published in Current Biology in 2018 (Freimer et al. 2018).

Results

Suppression of miRNA function in maturing oocytes is conserved.

MicroRNAs (miRNAs) and endogenous siRNAs (endo-siRNAs) represent two types of small RNAs that are defined by their differential biogenesis (Babiarz & Blelloch 2009). MiRNAs and endo-siRNAs form a complex with one of four Argonaute proteins (AGO1-4); the resulting complex then binds the 3' UTR of target mRNAs through either partial or complete complementation. Partial complementation of an AGO-small RNA complex with a target mRNA leads to the recruitment of additional proteins that inhibit translation and destabilize the transcript through exonucleolytic decay (Fabian & Sonenberg 2012; Bartel 2009). In contrast, perfect or near-perfect complementation of an AGO2-small RNA complex with a target mRNA, results in AGO2 endonucleolytic cleavage of the mRNA target (Liu et al. 2004). Genetic studies show that endo-siRNAs and the endonucleolytic activity of AGO2 are essential for oocyte maturation, while miRNAs are not (Murchison et al. 2007; Tang et al. 2007; Stein et al. 2015; Kaneda et al. 2009; Suh et al. 2010). Furthermore, removal of miRNAs has no discernable effect on the transcriptome of mouse oocytes, in striking contrast to other mouse cell types (Shenoy & Blelloch 2014; Suh et al. 2010).

To identify potential mechanisms underlying this surprising result, we first asked whether the loss of miRNA-driven translational repression and exonucleolytic destabilization is conserved across vertebrate species. To differentiate endonucleolytic cleavage from translational repression and exonucleolytic destabilization by small RNAs, we built renilla luciferase reporters carrying either a perfect match or four bulge sites to the miRNA, miR-15a (Figure 1A, 2). MiR-15a is highly conserved across *Xenopus laevis* (henceforth referred to as Xenopus), mouse, and human and is one of the most highly expressed miRNAs in oocytes (Kozomara & Griffiths-Jones 2014; Ma et al. 2010). We used firefly luciferase to normalize reporter activity. The ability of the reporters to readout both types of miR-15a activity was first

confirmed in 293T cells, where both perfect match and bulge reporters showed strong

suppression in presence of miR-15a (Figure 1B).

Next, these reporters were introduced into growing and GV/MII stage Xenopus oocytes.

Since transcription is silenced in oocyte development, the reporters were in vitro transcribed,

polyadenylated, and then injected. Similar to the 293T cells, growing Xenopus oocytes (stages

II-IV) showed a strong repression of both reporters, which was further enhanced with

co-injection of exogenous miR-15a (Figure 1C). However, once Xenopus oocytes had matured

to the GV stage (stage VI), suppression of the bulge reporter was absent even when co-injected

with miR-15a (Figure 1D). In contrast, knockdown of the perfect match reporter persisted.

Repression of the bulge reporter was absent through oocyte maturation to MII stage eggs in

Xenopus (Figure 1E). These results were similar to findings previously described for let-7 and

miR-30 in early growing versus fully grown GV/MII mouse oocytes (Ma et al. 2010). To pinpoint

when translational repression is lost during oocyte development, we performed a time course

analysis throughout early postnatal development in mice. Loss of translational repression began

between postnatal day 17 and 18 (Figure 1F), just prior to the loss of transcription in mouse

oocytes (Abe et al. 2010). Together, these results show a conserved loss in the ability of small

RNAs that imperfectly bind their targets to drive translational repression of reporters following

the transition from growing to maturing oocytes.

Exogenous hAGO2 and miRNA can rescue translational suppression of a reporter.

One possible explanation for the failure of GV and MII oocytes to suppress the bulge

reporter is that there are rate-limiting amounts of AGO2, enough for endonucleolytic cleavage,

but not translational repression and exonucleolytic destabilization. We performed

RNA-sequencing on mouse GV oocytes, and saw that full length *Ago2* is lowly expressed.

Surprisingly, *Ago2* is predominantly expressed as an unannotated truncated isoform which is not present in mouse embryonic stem cells (ESCs) (Figure 3A). RT-qPCR confirmed the presence of this isoform in oocytes and its absence in ESCs (Figure 4A). Additionally, RNA-Seq showed that *Ago1*, *Ago3*, and *Ago4* were also lowly expressed in mouse GV oocytes (Figure 3B). Since the four AGO proteins are functionally equivalent for translational suppression, we decided to focus primarily on AGO2 (Su et al. 2009). To directly test whether AGO was rate-limiting for translational repression, we injected in vitro transcribed full-length human *Ago2* (*hAgo2*) mRNA together with exogenous miR-15a and the bulge reporter. This approach showed a robust and reproducible repression of the reporter in both Xenopus and mouse GV oocytes (Figure 3C, D). The exogenous hAGO2 had no effect on a reporter without bulge sites (Figure 4B, C). Surprisingly, a mutant form of hAGO2 with 10 mutations in the PAZ domain (Liu et al. 2005), which has been shown not to bind miRNAs, was also able to rescue suppression of the reporter when injected together with exogenous miR-15a (Figure 3C, D). However, recent data suggests that this mutant likely retains some low-level activity, which in the context of overexpression may be enough to re-activate function (Gu et al. 2012). These data show that exogenous hAGO2 can restore small RNA driven translational repression of an exogenously introduced reporter in maturing Xenopus and mouse oocytes.

Since small RNA-induced endonucleolytic cleavage is vital in mouse oocytes, we considered the possibility that translational repression may be suppressed due to competition for AGO by the large number of endo-siRNAs (Tam et al. 2008; Watanabe et al. 2008). To test this possibility, we repeated the luciferase assays in DICER knockout oocytes, which lack all endogenous siRNAs and miRNAs (Suh et al. 2010). Even in the absence of endogenous small RNAs, exogenous miR-15a was not sufficient to knockdown the reporter (Figure 3E). Robust

repression was only observed with both exogenous hAGO2 and miRNA (Figure 3E), suggesting

that endo-siRNAs sequestering AGO2 is not the reason for the loss of translational repression.

MiRNAs can both repress the translation of their mRNA targets and destabilize them

through exonucleolytic decay (Jonas & Izaurralde 2015). The predominant mechanism of action

is believed to be context dependent (Alemán et al. 2007; Bazzini et al. 2012; Eichhorn et al.

2014; Jonas & Izaurralde 2015; Subtelny et al. 2014). Reduced luciferase activity could be due

to either mechanism. To determine whether overexpression of hAGO2 affected Renilla mRNA

levels, we performed RT-qPCR on injected Renilla and Firefly mRNA. While overexpression of

hAGO2 and exogenous miR-15a reduced Renilla mRNA levels in 3 of 4 experiments (Figure

4D), the combined results did not reach significance and the effect was small, suggesting that

the primary mechanism behind the reduced luciferase levels is translational repression.

Exogenous AGO2 and miRNA have a minimal impact on endogenous targets.

To identify the developmental and molecular consequences of re-activating translational

repression in the oocyte, we turned to a genetic system in the mouse where exogenous full

length hAGO2 is expressed from the Rosa26 promoter following Cre-mediated excision

(R26-lox-stop-lox-GFP-myc-hAGO2) (He et al. 2012). We crossed this mouse to an oocyte

specific Cre (Zp3-Cre) to drive oocyte specific overexpression of full length hAGO2 (de Vries et

al. 2000). RT-qPCR showed a 10-fold increase in expression of total *Ago2* expression in

Cre-positive GV oocytes (Figure 5A). This increase in expression alone did not repress the

bulge reporter (Figure 5B). Similarly, exogenous miR-15a alone induced only a slight and

inconsistent downregulation (Figure 5C). However, the two together showed robust knockdown

of the bulged reporter (Figure 5D), similar to that seen with injection of the exogenous AGO2

mRNA along with miRNA.

Next, we asked how this system affects the endogenous transcriptome. We performed microarray profiling on both control and Rosa26 driven hAGO2-overexpressing mouse GV oocytes. Only 3 genes were differentially expressed at a false discovery rate (FDR) < 0.05, including *Ago2* itself (Figure 5E). These findings are consistent with the reporter data showing that hAGO2 overexpression alone failed to rescue suppression. Surprisingly though, hAGO2 overexpression along with exogenous miR-15a injection also had very little impact on the transcriptome (Figure 5F). 29 genes were down-regulated with a FDR < 0.05, while 3 genes were stabilized (i.e. 'up-regulated') including *Ago2* itself. We further evaluated the 29 down-regulated genes to determine if they were enriched for miR-15a targets. Of 1121 conserved targetscan miR-15a targets, 778 are found on the array and 444 are expressed in oocytes, but only 1 was among the down-regulated genes. Biological replicates were well correlated, and thus the lack of changes is not due to noise between replicates (Figure 6). These findings show that exogenous hAGO2-miRNA complexes have little effect on the transcriptome of oocytes either through destabilization of direct miR-15a targets or through indirect targets which would likely be altered due to translational changes of miR-15a targets. This finding suggests that AGO2 levels alone are unlikely to explain the loss of miRNA activity in maturing oocytes.

Isoforms with longer 3' UTRs are more stable in maturing oocytes.

An additional mechanism of suppressing miRNA activity could occur at the level of the target transcript. Alternative polyadenylation (APA) produces 3' UTRs of differing lengths (Elkon et al. 2013). In somatic cells, a shorter 3' UTR is generally associated with greater mRNA stability, at least in part due to a decrease in the number of miRNA target sites (Sandberg et al. 2008; Spies et al. 2013; Mayr & Bartel 2009). Therefore, we evaluated alternative

polyadenylation usage during the GV to MII transition. Hundreds of transcripts showed

differential 3' UTR length during the GV to MII transition (Figure 7A, B). For comparison, we

looked at an alternative transition, the embryonic stem cell (ESC) to epiblast like cell (EpiC)

transition, a time of abundant miRNA activity (Gu et al. 2016). There were very few changes in

3' UTR length during this transition (Figure 7C, D). Surprisingly, the changes in the maturing

oocyte showed a strong enrichment for distal polyadenylation usage in MII versus GV oocytes

(Figure 7B vs. 7D). Four hundred and sixty-three genes showed preferential stability of

transcripts using the distal polyadenylation site (median 4.3 fold increase in 3' UTR length) while

one hundred and twenty-nine genes showed preferential stability of transcripts using the

proximal polyadenylation site (median 2.8 fold decrease in 3' UTR length) (Figure 7E). Individual

tracks for the Pafah1b1 and Srp1k genes exemplified the striking switch between short and long

forms between GV and MII oocytes (Figure 7F). Many of the 3' UTRs gained during the GV to

MII transition had target sites for miR-15a, but were not impacted by introduction of exogenous

miR-15a and AGO2 (Figure 7F). Given the absence of transcription during the GV to MII

transition, these changes must reflect the preferential degradation of the short 3' UTR isoforms,

directly contrasting the previous findings in non-oocyte populations, where the long isoforms

were preferentially degraded (Mayr & Bartel 2009; Sandberg et al. 2008; Spies et al. 2013).

Thus, preferential expression of short 3' UTR isoforms does not underlie the resistance of

maturing oocytes to miRNA driven exonucleolytic decay.

<u>Discussion</u>

In this study, we sought to uncover the mechanism underlying the surprising finding that

miRNA function is absent during oocyte maturation, a discovery originally made in mouse

oocytes (Ma et al. 2010; Suh et al. 2010). Here, we show that translational repression is also

absent in maturing Xenopus oocytes, showing conservation across vertebrates. In both species, translational repression was suppressed around the transition from oocyte growth to maturation. Furthermore, in both species, the introduction of exogenous hAGO2 and miRNA were able to rescue repression of reporter constructs. Recent studies have shown that miRNA levels and AGO levels are intimately connected; each stabilizing the other (Zamudio et al. 2014; Martinez & Gregory 2013). This mutual dependency could explain why introducing both together is necessary for robust knockdown.

In mouse oocytes, RNA-Sequencing showed that *Ago2* predominantly exists as a truncated form of AGO2 missing the PAZ, MID, and PIWI domains, making it highly unlikely that it retains activity (Song et al. 2004). The low levels of full length AGO2 may be enough for the observed endonucleolytic cleavage, but not translational repression. Indeed, slicing is a more efficient process than translational repression and thus likely to require significantly less AGO2 (Ebert et al. 2007). Alternatively, truncated AGO2 might act as a dominant negative, but overexpression of the truncated form in 293Ts did not negatively impact repression (Figure 8A). Therefore, the most likely explanation is that low levels of full length AGO2 contributes to the loss of miRNA induced repression.

However, this mechanism alone does not fully explain the lack of miRNA repression in oocytes. Even in the presence of exogenous AGO2 and miRNAs, there was minimal degradation of luciferase mRNA. This finding contrasts the effects seen in somatic cells where exonucleolytic decay plays a predominant role in the inhibition of target mRNAs (Eichhorn et al. 2014). In addition, expression profiling showed that endogenous targets of miR-15a were not destabilized at the transcript level upon introduction of exogenous AGO2 and miR-15a. Furthermore, there was a near absence of transcriptional changes globally. While it is possible that miRNAs solely repress translation in this context, the altered translation of hundreds of

miR-15a targets would be expected to produce secondary mRNA changes. Therefore, additional mechanisms are likely blocking miRNA function in oocytes.

The nature of additional mechanisms that could underlie the global suppression of miRNA activity in oocytes is unclear. However, additional effectors of miRNA activity are also lowly expressed in the oocyte. Most notably, several proteins involved in exonucleolytic decay including Xrn1, the primary 5' to 3' exonuclease downstream of miRNA activity, are also lowly expressed in oocytes (Figure 8B). Furthermore, components of the deadenylation and decapping complexes are lowly expressed and minimally active in GV oocytes (Ma et al. 2015; Ma et al. 2013). The reduced exonucleolytic activity could also explain the previously described persistence of RNA fragments in oocytes (Svoboda et al. 2015). Recent work has also shown that post-translational modifications of AGO2 are essential for normal function (Golden et al. 2017). In particular, cycles of phosphorylation and dephosphorylation are essential for optimal activity. Future measurements of the activities of the kinase and phosphatase responsible for these cycles could uncover a potential role for these factors in the loss of miRNA activity in maturing oocytes.

Another potential mechanism to avoid miRNA function would be preferential expression of transcript isoforms with short 3' UTRs reducing the number of potential miRNA targeting sites. However, in contrast to previous work on non-oocytes (Mayr & Bartel 2009; Sandberg et al. 2008; Spies et al. 2013), we found that longer 3' UTRs are associated with increased rather than decreased stability of the cognate transcript during oocyte maturation. This finding suggests inhibition of miRNA function upstream of the target transcript. How longer 3' UTRs stabilize transcripts in the oocyte is unclear. It is possible that the binding of stabilizing RNA binding proteins (RBPs) to the 3' UTRs in the absence of miRNA activity underlies this stabilization and might even serve as a redundant mechanism to prevent miRNA activity.

Indeed, oocytes express many RBPs that bind the 3' UTRs of transcripts to promote cytoplasmic polyadenylation, which in turn promotes stabilization, or that directly antagonize miRNA function (Racki & Richter 2006; Kedde et al. 2007; Jonas & Izaurralde 2015; Kedde et al. 2010). Thus, the longer 3' UTRs could provide docking sites for these RBPs, which in turn suppresses degradation of the cognate mRNA.

In summary, we have identified an alternative truncated isoform of AGO2, which is the dominant AGO species in maturing oocytes. Re-introduction of full-length hAGO2 together with an exogenous miRNA represses reporters in a setting where endogenous miRNA function is absent. However, endogenous transcripts are still resistant to miRNA driven exonucleolytic activity. Therefore, there appear to be multiple mechanisms of globally suppressing miRNA activity in the maturing vertebrate oocyte, one of which is a dramatic reduction in the levels of functional AGO-miRNA complexes.
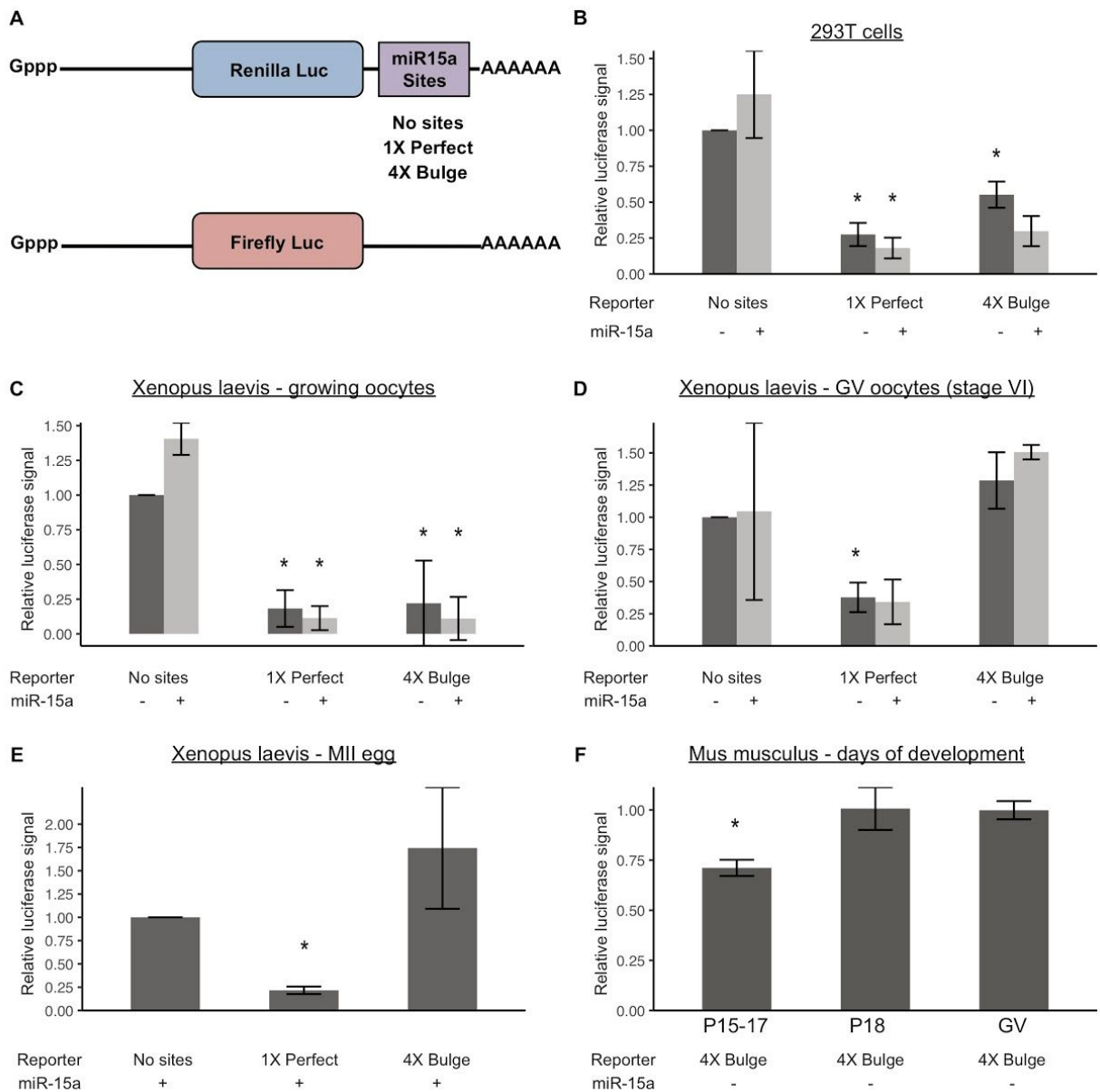
Figure 1 – Suppression of miRNA activity in maturing oocytes is conserved from mouse to Xenopus.
A) Schematic of constructs used in all subsequent luciferase assays. miR-15a sites were cloned in the 3' UTR of Renilla luciferase (Luc) - either a 1X site with a perfect match or a 4X site with a bulged match to miR-15a. A control of no sites was also used. Firefly luciferase was used as an injection control. All injected transcripts were transcribed, capped, and polyadenylated in vitro.
B) Luciferase assay in HEK-293T cells transfected with or without miR-15a mimic and

psiCHECK2, a vector containing Firefly luciferase and Renilla luciferase with either no miR-15a sites, 1X Perfect, or 4X Bulge sites in the 3' UTR of Renilla luciferase. N=2. C,D) Luciferase assays in Xenopus laevis (C) growing (stage III-V) and (D) GV (stage VI), using 1X Perfect and 4X Bulge templates, with or without miR-15a mimic. N=2. E) Luciferase assay as in (B), but in Xenopus MII eggs, with miR-15a mimic. N=2. F) Luciferase assays in oocytes at various stages of postnatal mouse development P15-23 (x-axis), with miR-15a mimic. For P15-17 N=4, P18 N=3, GV (P23) N=4. All luciferase data is a ratio of Renilla signal over Firefly signal. All error bars represent standard deviation. Asterisks (*) represent significantly different data from the corresponding 'No sites' control data, except in F) where they represent significantly different data from GV (Student's T-test, $p<0.05$).

miR-15a   3' – guguuugguaauacacgacgau – 5'
                      | | | | | | | | | | | | | | | | | | | | |
miR-15a perfect match UTR   5' …cacaaaccauuaugugcugcua… 3'

miR-15a   3' – guguuugguaauacacgacgau – 5'
                      | | | | | | | | | | | | | | | | | |
miR-15a bulge match UTR   5' …cacaaaccau--cagugcugcua… 3'
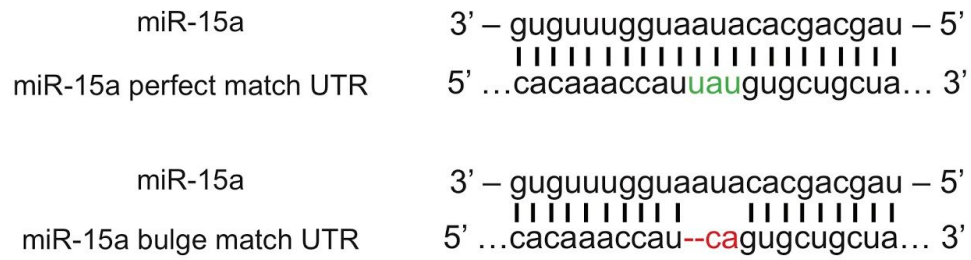
Figure 2 - Schematic of reporter UTRs.
Schematic of reporter UTR sequences illustrating miR-15a binding to the perfect and bulge sequences in the 3' UTR of Renilla luciferase.
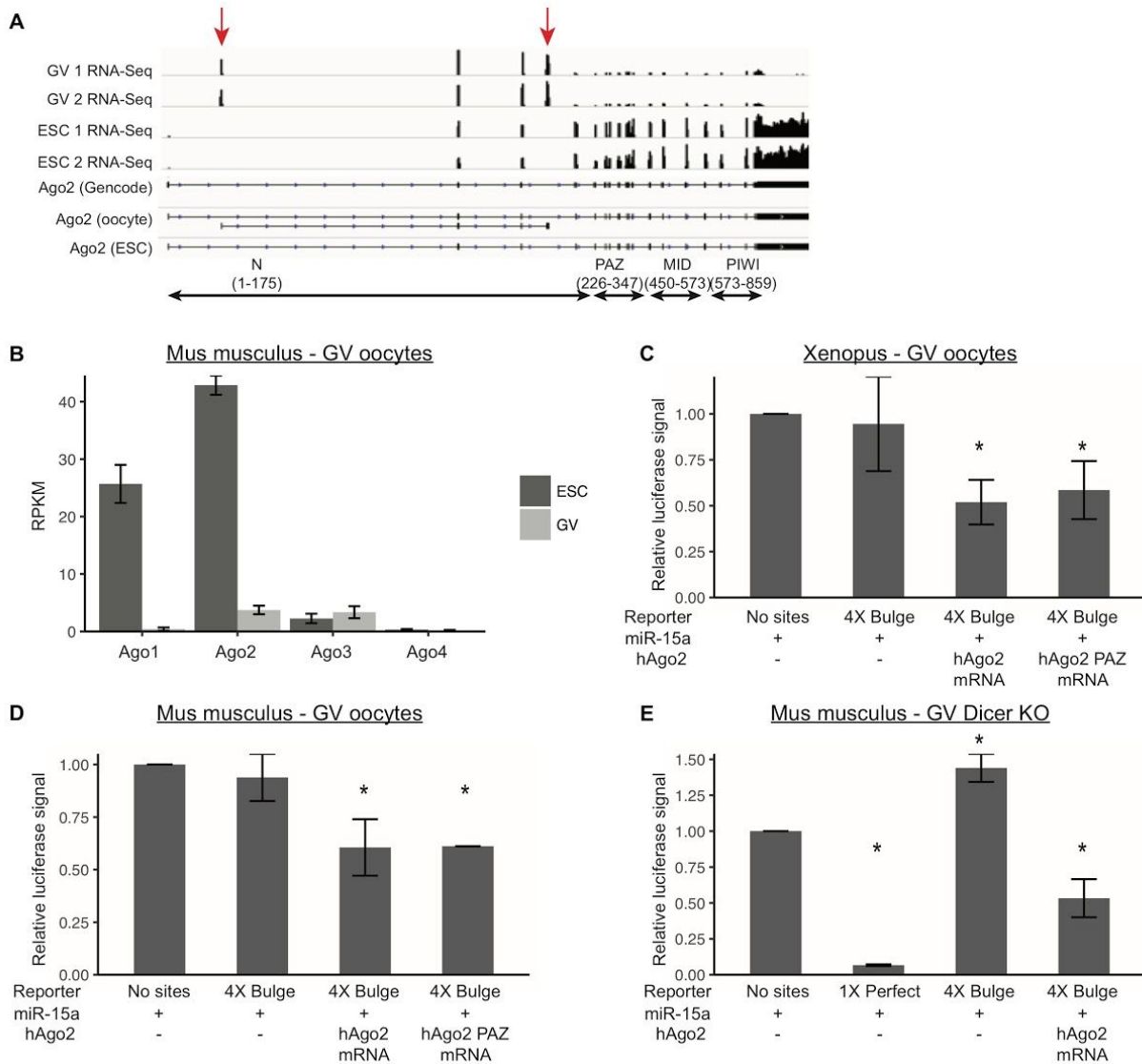
Figure 3 – Exogenous hAGO2 and miRNA can rescue translational suppression of a reporter.

A) RNA-Seq coverage of *Ago2* isoforms in mouse GV oocytes and embryonic stem cells. Lower tracks represent Gencode *Ago2* isoform and Stringtie reconstructed isoforms in oocytes and embryonic stem cells. Arrows denote exons present only in the oocyte isoform. B) RNA-Seq in mouse GV oocytes and mouse ESCs showing expression of the four *Ago* proteins. C, D) Luciferase assays in (C) Xenopus GV oocytes or (D) mouse GV oocytes with injection of miR-15a mimic and either wild-type hAGO2 or hAGO2-PAZ10 mutant mRNA. C, N=10; D, AGO2 N=7, PAZ10 N=2. E) Luciferase assays in DICER KO mouse GV oocytes, with miR-15a mimic and either a 1X Perfect or 4X Bulge template, with or without addition of hAGO2. N=2. Luciferase data is a ratio of Renilla signal over Firefly signal. All error bars represent standard deviation. Asterisks (*) represent significantly different data from the corresponding 'No sites' control data (Student's T-test, p<0.05).
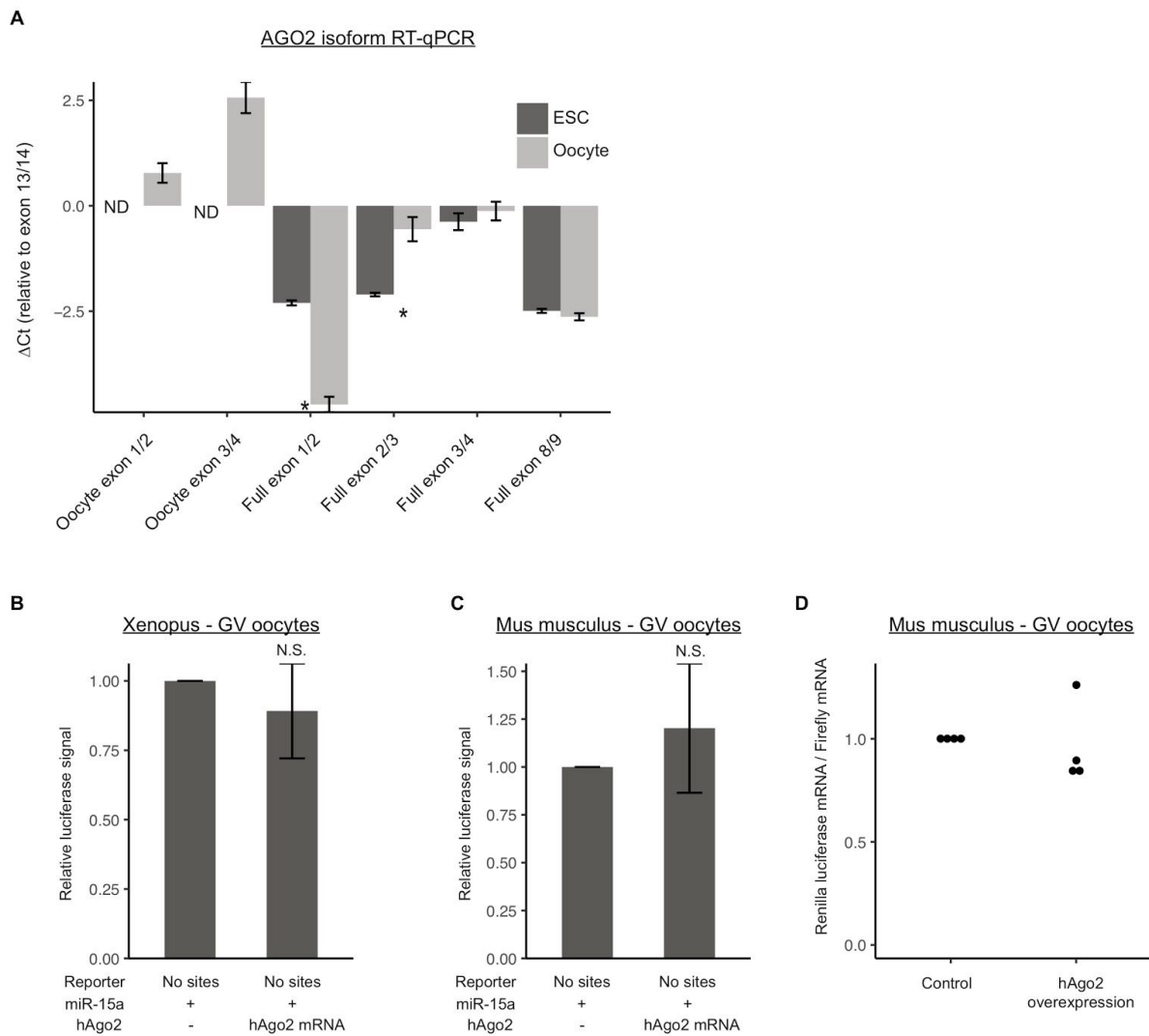
Figure 4 – Characterization of Oocyte-specific Ago2 isoform.
A) RT-qPCR with primers spanning exons in full length or oocyte specific AGO2. Data is ΔCt in embryonic stem cells and GV oocytes relative to primers spanning exon 13/14. Embryonic stem cell N=2, oocyte N=3. ND = Not detected. Asterisks (*) represent significantly different data from the corresponding 'ESC' control data (Student's T-test, p<0.05). Luciferase assays in (B) Xenopus GV oocytes or (C) mouse GV oocytes following injection of miR-15a mimic, reporter lacking target sites, plus and minus wild type AGO2 mRNA. N=10 for B, N=2 for C. D) RT-qPCR for Renilla 4x bulge and Firefly in either control (WT or LSL-GFP-myc-hAgo2/+; Zp3-Cre-) or AGO2 overexpressing (injected with AGO2 mRNA or LSL-GFP-myc-hAGO2/+; Zp3-Cre+) mouse GV oocytes along with miR-15a mimic. Dots represent biological replicates. N=4. All error bars represent standard deviation. N.S. = not significant.
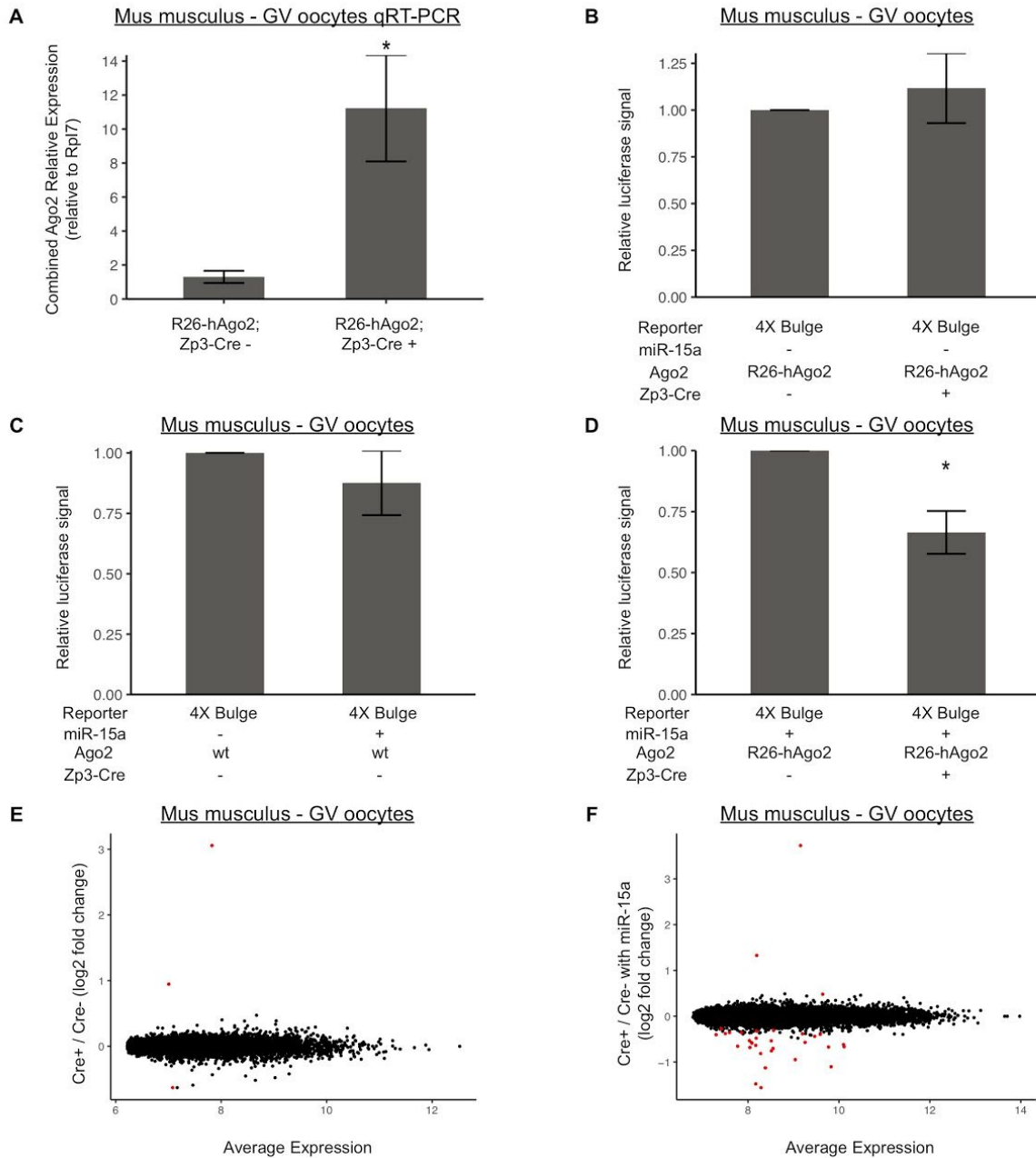
Figure 5 – Both Exogenous hAGO2 and miRNA are required to rescue miRNA activity, but have minimal impact on endogenous targets.

A) RT-qPCR of combined mouse and human *Ago2* mRNA levels in LSL-GFP-myc-hAGO2/+; Zp3-Cre+ and Zp3-Cre- mouse GV oocytes. Primers recognize both mouse and human AGO2. Rpl7 is used as a reference gene. N=4. B) Luciferase assay in LSL-GFP-myc-hAGO2/+; Zp3-Cre+ and Zp3-Cre- mouse GV oocytes with no miR-15a mimic and 4x Bulge template. N=2. C) Luciferase assay in wild type mouse GV oocytes with miR-15a mimic and 4x Bulge template. N=4. D) Luciferase assay in LSL-GFP-myc-hAGO2/+; Zp3-Cre+ and Zp3-Cre- mouse GV oocytes with miR-15a mimic and 4x Bulge template. N=3. Illumina Bead Array RNA profiling of: E) LSL-GFP-myc-hAGO2/+; Zp3-Cre+ versus Zp3-Cre- mouse GV oocytes. F)

24

LSL-GFP-myc-hAGO2/LSL-GFP-myc-hAGO2; Zp3-Cre+ versus Zp3-Cre- mouse GV oocytes injected with miR-15a mimic. Significant differentially expressed transcripts shown in red (FDR < 0.05). E, N=3; F, N=4. Data is a ratio of Renilla signal over Firefly signal. All error bars represent standard deviation. Asterisks (*) represent significantly different data from the corresponding control data (Student's T-test, p<0.05).
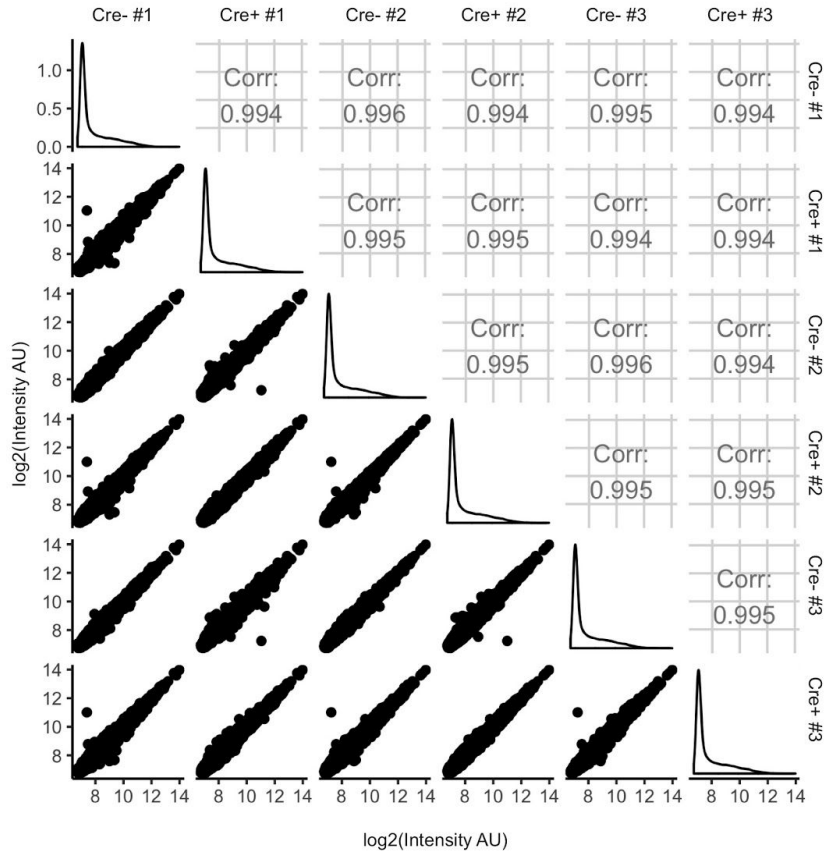
Figure 6 – Correlations between arrays.
A) Log2 quantile normalized intensity values between replicates of
LSL-GFP-myc-hAGO2/LSL-GFP-myc-hAGO2; Zp3-Cre+ and Zp3-Cre- mouse GV oocytes
injected with miR-15a mimic.
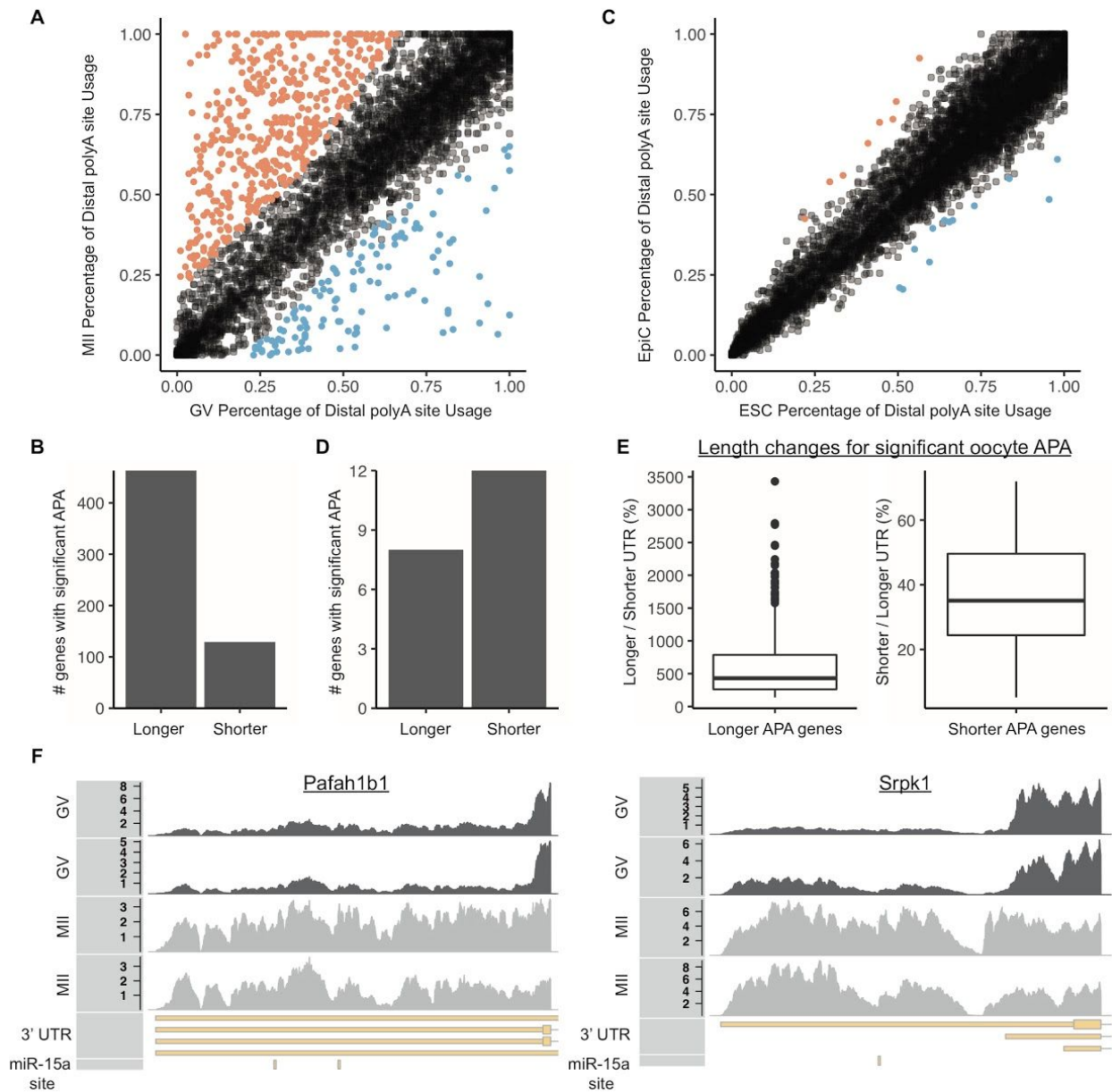
Figure 7 - Isoforms with longer 3' UTRs are more stable in maturing oocytes.
(A) Percentage of distal alternative polyadenylation site usage in GV and MII oocytes.
Significant increases in distal alternative polyadenylation usage are colored in orange,
significant decreases are colored in blue. Each dot represents one gene. (B) Number of
significant changes in alternative polyadenylation ratios resulting in longer 3' UTRs or shorter 3'
UTRs during the GV to MII transition. (C) Same as A, except in mouse ESCs and EpiCs. (D)
Same as B, except in mouse ESCs and EpiCs. (E) Boxplots showing change in 3' UTR length
for genes with a significant change in alternative polyadenylation during the GV to MII transition.
Left plot shows the ratio of the longer 3' UTR relative to the shorter 3' UTR for genes where the
distal polyadenylation site is more stable (n = 463 genes). Right plot shows the ratio of the
shorter 3' UTR relative to the longer 3' UTR for genes where the proximal polyadenylation site is
more stable (n = 129 genes). (F) RNA-Seq coverage showing stabilization of distal alternative

polyadenylation site in GV to MII transition at two genes (Pafah1b1 and Srpk1). Both genes are on the negative strand (transcribed from right to left). 2 GV replicates, 2 MII replicates, Gencode annotated 3' UTR, miR-15a TargetScan predicted target site.
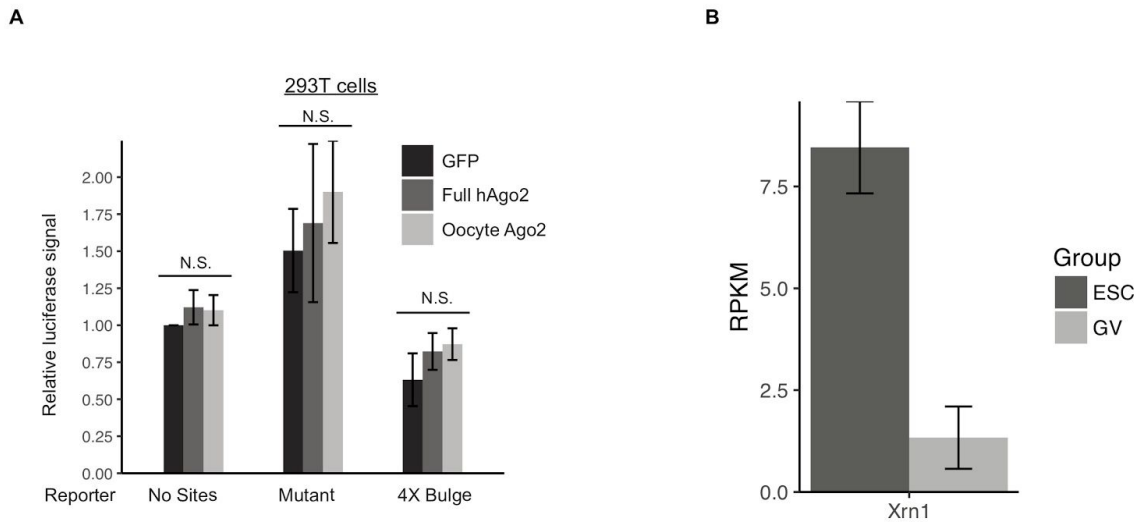
Figure 8 – Evaluation of additional potential mechanisms that impact miRNA activity.
A) Luciferase assay in HEK-293T cells transfected with psiCHECK2, a vector containing Firefly luciferase and Renilla luciferase with either no let-7 sites, mutated sites, or 4X bulge sites in the 3' UTR for Renilla luciferase. psiCHECK2 was co-transfected with either GFP, full length hAGO2, or truncated oocyte AGO2. Luciferase data is a ratio of Renilla signal over Firefly signal. Full and truncated AGO2 is not significantly different from GFP control in all cases. All error bars represent standard deviation. N.S. = not significant. B) RNA-Seq expression of Xrn1 in mouse embryonic stem cells and mouse GV oocytes.

Methods

EXPERIMENTAL MODEL AND SUBJECT DETAILS

R26-hAGO2 mice

Rosa26 lox-stop-lox-myc-GFP-hAGO2 (R26-hAGO2) mice (He et al. 2012) were obtained from the Jackson Laboratory (JAX stock #017626). These mice were crossed to C57/B6 Zp3-Cre mice (de Vries et al. 2000) to generate R26-hAGO2; Zp3-Cre mice. For all experiments, R26-hAGO2; Zp3-Cre- females were bred to R26-hAGO2; Zp3-Cre+ males. Oocytes were collected from 3-4 week old female Cre- and Cre+ littermates. Mice were housed per UCSF and IACUC guidelines.

Wild Type mice

C57/B6 mice were ordered from the Jackson Laboratory (JAX stock #00064) and Simonsen Laboratory (Stock #C57BL/6NCrSim). Oocytes were collected from 3-4 week old females.

Xenopus laevis

Mature female Xenopus laevis were ordered from Nasco (Stock #LM00535MX) and cared for per supplier instructions and IACUC guidelines. Mature females were staged by length (9+ cm) according to Nasco instructions.

Cell lines and cell culture

293Ts were grown in DMEM supplemented with 10% Fetal Bovine Serum. ESCs were grown in Knockout DMEM (Invitrogen) supplemented with 15% Fetal Bovine Serum, LIF and 2i (PD0325901 and CHIR99021). To generate Epi cells, ESCs were plated at 400,000 cells in a 15 plate, 24 hours later LIF and 2i were removed and Epi Cells were collected ~56 hours later

(Krishnakumar et al. 2016). ESCs are male. 293Ts are female. ESC lines were authenticated

via RNA-Seq.

METHOD DETAILS

Constructs

miRNA binding sites were ordered as oligos from IDT. Oligos were phosphorylated, annealed,

and cloned into the 3' UTR of psiCHECK2 (Promega) using the restriction enzymes NotI and

XhoI. Truncated AGO2 was amplified from oocyte cDNA and cloned into pGAMA. Full length

hAGO2 was amplified from an existing plasmid and cloned into pGAMA.

Primers

Let7Perfect Sense	TCGAATAAACTATACAACCTACTACCTCC
Let7Perfect Anti	GGCCGGAGGTAGTAGGTTGTATAGTTTAT
Let7Bulge Sense1	TCGAATAAACTATACACATACTACCTCCGATACTATACACATACTACCTCACGCGT
Let7Bulge Sense2	ACTATACACATACTACCTCTCACACTATACACATACTACCTCC
Let7Bulge Anti1	GGCCGGAGGTAGTATGTGTATAGTGTGAGAGGTAGTATGTGTATAGTACGCGT
Let7Bulge Anti2	GAGGTAGTATGTGTATAGTATCGGAGGTAGTATGTGTATAGTTTAT
Let7Mutant Sense1	TCGAATAAACTATACACATAATCCATCCGATACTATACACATAATCCATCACGCGT
Let7Mutant Sense2	ACTATACACATAATCCATCTCACACTATACACATAATCCATCC
Let7Mutant Anti1	GGCCGGATGGATTATGTGTATAGTGTGAGATGGATTATGTGTATAGTACGCGT
Let7Mutant Anti2	GATGGATTATGTGTATAGTATCGGATGGATTATGTGTATAGTTTAT
miR15Perfect Sense	TCGAATAACACAAACCATTATGTGCTGCTAC
miR15Perfect Anti	GGCCGTAGCAGCACATAATGGTTTGTGTTAT
miR15Bulge Sense1	TCGAATAAcacaaaccatCAgtgctgctaCGATcacaaaccatCAgtgctgctaACGCGT
miR15Bulge Sense2	cacaaaccatCAgtgctgctaTCACcacaaaccatCAgtgctgctaC
miR15Bulge Anti1	GGCCGTAGCAGCACTGATGGTTTGTGGTGATAGCAGCACTGATGGTTTGTGACGCGT
miR15Bulge Anti2	TAGCAGCACTGATGGTTTGTGATCGTAGCAGCACTGATGGTTTGTGTTAT
miR15Mutant Sense1	TCGAATAACACAAACCATCAGTTCGGATACGATCACAAACCATCAGTTCGGATAACGCGT

miR15Mutant Sense2	CACAAACCATCAGTTCGGATATCACCACAAACCATCAGTTCGGATAC
miR15Mutant Anti1	GGCCGTATCCGAACTGATGGTTTGTGGTGATATCCGAACTGATGGTTTGTGACGCGT
miR15Mutant Anti2	TATCCGAACTGATGGTTTGTGATCGTATCCGAACTGATGGTTTGTGTTAT
Rosa26 Ago2 common genotyping	CCAAAGTCGCTCTGAGTTGTTATC
Rosa26 Ago2 WT RVS genotyping	GAGCGGGAGAAATGGATATG
Rosa26 Ago2 MUT RVS genotyping	CGGGCCATTTACCGTAAG
Cre genotyping FWD genotyping	tgggcggcatggtgcaagtt
Cre genotyping RVS genotyping	cggtgctaaccagcgttttc
Il2 genotyping FWD genotyping	ctaggccacagaattgaaagatct
Il2 genotyping RVS genotyping	gtaggtggaaattctagcatcatcc
RPL7 qPCR FWD	gattgtggagccatacattgca
RPL7 qPCR RVS	tgccgtagcctcgcttgt
mouse human Ago2 qPCR FWD	ctcacctggtggccttcc
mouse human Ago2 qPCR RVS	agaggtatggcttccttcagc
Oocyte Exon 1 - Exon 2	AGAATCCTTCCTGCCTTCCTTC
Oocyte Exon 1 - Exon 2	TTGAAGGCATATCCTGGGATGG
WT Exon 2 - Exon 3	GGACATCAAACCTGAGAAATGCC
WT Exon 2 - Exon 3	TCCATCAAACACTGGCTTCC
Oocyte Exon 3 - Exon 4	TACACAGCAATGCCCCTTCC
Oocyte Exon 3 - Exon 4	CAGTTCATGCTTCTGCTCTTGC
WT Exon 1 - Exon 2	GCAACGCCACCATGTACTC
WT Exon 1 - Exon 2	TTGAAGGCATATCCTGGGATGG
WT Exon 3 - Exon 4	AGCCAGTGTTTGATGGAAGG
WT Exon 3 - Exon 4	ATGCGATCTTTGCCTTCTCC
WT Exon 8 - Exon 9	cagacaatcagacctcaaccatg
WT Exon 8 - Exon 9	cacttcgcatcagtttgctg

WT Exon 13 - Exon 14	acagaccctatccaatctctgc
WT Exon 13 - Exon 14	atgacaggttgctggaacac
Renilla qPCR FWD	ACGCAAACGCATGATCACTG
Renilla qPCR RVS	GCAGAAAAATCACGGCGTTC
Firefly qPCR FWD	CGTGCCAGAGTCTTTCGACA
Firefly qPCR RVS	ACAGGCGGTGCGATGAG

In vitro transcription

Linearized psiCHECK2 vector (Promega), pCDNA3-myc-hAGO2 (Liu et al. 2004), or

pCDNA3-RFP was in vitro transcribed and capped (Ambion). mRNA was then polyadenylated

by Poly(A) tailing kit (Ambion).

Mouse oocyte collection and injection

48 hours prior to injection mice were primed with 5 units of PMSG. GV oocytes were collected in

MEM medium supplemented with 2uM milrinone to prevent resumption of meiosis. *In vitro*

transcribed mRNA and 2uM miR-15a mimic (Dharmacon) were injected on a Leica DMI3000 B

with an Eppendorf FemtoJet. Oocytes were cultured in MEM medium supplemented with 2uM

milrinone overnight at 37˚ and 5% CO2 for luciferase assays.

Luciferase assay

Luciferase assays were performed using the Dual Luciferase Reporter Assay kit (Promega) and

measured on a SpectraMaxL Luminometer (Molecular Devices). Renilla signal was normalized

to firefly signal for all experiments.

Microarray

RNA was extracted from GV oocytes with the PicoPure RNA Isolation Kit (ARCTURUS). RNA was sent to the UCLA Neuroscience Genomics Core where cDNA was amplified (Nugen) and then hybridized to Illumina BeadChips. Data was pre-processed and normalized in R version 3.3.2 using bead array version 2.24.0 (Dunning et al. 2007). Differential expression was performed in R using limma version 3.30.4 (Ritchie et al. 2015).

AGO2 RT-qPCR

RNA was extracted with TRIzol (Invitrogen). cDNA was made using Superscript III First-strand Synthesis kit (Invitrogen) following the standard protocol. qPCR was performed using Power SYBR Green mix (Applied Biosystems) on an ABI 7900HT 384-well PCR machine.

Luciferase RT-qPCR

RNA was extracted with PicoPure RNA Isolation Kit (ARCTURUS). cDNA was made using Maxima RT cDNA kit (Thermo Scientific) following the standard protocol. qPCR was performed using Roche SYBR Green mix (Roche) on an ABI 7900HT 384-well PCR machine.

RNA-Seq

RNA from GV oocytes and mouse embryonic stem cells was extracted in TRIzol (Invitrogen) and sequencing libraries were made using the Illumina stranded paired-end Truseq kit (Illumina). Reads were mapped to the mm10 mouse genome using STAR version 2.5.1b (Dobin et al. 2013). Reads were counted with featureCounts (Liao et al. 2014) version 1.5.0-p1 using the Gencode m10 genome annotation. De novo isoform discovery was performed in stringtie version 1.2.4 (Pertea et al. 2015).

Transfections

All transfections were done in 96 well plates with 200 ng of DNA following the standard Fugene 6 (Promega) protocol.

Xenopus oocyte collection and injection

To prepare Xenopus laevis for surgery, animals were anaesthetized using a 2 grams/liter solution of tricaine methane sulfonate (MS-222) buffered to a neutral pH of 7.0-7.5 using sodium bicarbonate. Autoclave-sterilized tools were used to perform live surgery, and oocytes were removed by biopsying the ovary (no more than 50%). The frogs were then re-sutured using nylon monofilament suture, and monitored in a shallow tank until they were fully awake and mobile. They were then returned to their housing tank, and observed daily for 3 days. Frogs were used for surgery only once every 3 months (or longer if necessary).

Once harvested, oocytes were dissociated in 2 mg/ml collagenase in modified Barth's saline (1X MBS) at room temperature for 1-3 hours, being constantly monitored to avoid over digestion. The oocytes were then transferred to culture media (10% fetal calf serum, 1X penicillin/streptomycin, 100 µg/mL gentamycin, 50% L-15 medium (Leibovitz) + glutamine) for subsequent procedures and incubations.

Xenopus oocytes were injected using a microINJECTOR system (Tritech research). Concentrations of materials injected were the same as for mouse oocytes (see above). For luciferase assays, oocytes were incubated overnight at 16C, and lysed (single oocytes in individual wells of a 96 well plate) using as directed in the Dual Luciferase Reporter Assay kit (see above).

For maturation of oocytes into eggs (MII), stage VI oocytes were incubated with 3uM progesterone in culture media overnight.

APA analysis

DaPars (Xia et al. 2014) version 0.9.1 was used to identify Percentage of Distal poly(A) site Usage Index (PDUI). DaPars was run with the default settings from the original paper describing the software: Adjusted P Value < 0.05, minimum ΔPDUI of 0.2, and minimum 1.5 fold change in PDUI. For genes with more than two transcripts and more than 2 ΔPDUI changes, the greatest ΔPDUI and lowest adjusted P value was used. Conserved miRNA target sites were downloaded from TargetScan 7.1.

Experimental Design

For all experiments n indicating the number of biological replicates are given in figure legends. The study was not done blinded. No data was excluded. Based on previous literature we assume luciferase data follows a t-distribution and use a t-test for calculating significance. Different litters were used for different biological replicates.

QUANTIFICATION AND STATISTICAL ANALYSIS

For all experiments n indicating the number of biological replicates and additional details are listed in the figure legend. For oocyte experiments, biological replicates refers to pools of oocytes collected on different days. For cell lines, biological replicates refers to separate culture dishes of cells. All luciferase data is a ratio of Renilla signal over Firefly signal. All error bars represent standard deviation. Asterisks (*) represent significant differences with student's T-test, $p < 0.05$. For array and sequencing analysis differences were defined with an adjusted P value < 0.05. Statistical significance was calculated in R version 3.3. To the extent possible, we checked if data met assumptions of statistical methods used.

Chapter 3 - Decoupling translation repression from mRNA degradation of miRNA targets

Summary

Translation and mRNA degradation are intimately connected, yet the mechanisms that regulate both are not fully understood. Here we examine the regulation of translation and mRNA stability in mouse embryonic stem cells (ESCs) and during differentiation. In contrast to previous reports, we found that transcriptional changes account for most of the molecular changes during ESC differentiation. However, within ESCs there was a positive correlation between translation level and mRNA stability. We asked if the RNA-binding protein DDX6 links these processes in ESCs since the yeast homolog of DDX6 connects codon optimality and mRNA stability. However there was minimal connection between codon usage and stability changes in DDX6 KO ESCs. DDX6 has also been implicated in microRNA mediated repression, a process involving both translational repression and mRNA destabilization. Surprisingly, the loss of DDX6 leads to the translational derepression of microRNA targets without affecting mRNA stability. Furthermore, DDX6 KO ESCs share overlapping phenotypes and global molecular changes with ESCs that completely lack all microRNAs. Together our results demonstrate that it is possible to decouple the two forms of microRNA induced repression and emphasize that the translational aspect of microRNA repression is underappreciated.

Introduction

Gene expression is determined through a combination of transcriptional regulation and post-transcriptional regulation. While transcriptional regulation has been extensively studied, less is known about how the regulation of mRNA stability affects overall mRNA levels. Mammalian mRNAs display a wide range of half lives ranging from minutes to over a day

(Schwanhäusser et al. 2011). However, many of the factors that control the frequency with which a transcript enters the degradation pathway are not well understood.

One process that is intimately linked to mRNA decay is translational repression (Roy & Jacobson 2013). Quality control mechanisms such as nonsense mediated decay, no go decay, and non stop decay sense aberrant translation and lead to degradation of the mRNA (Parker 2012; Shoemaker & Green 2012). Additionally, translational repression and RNA decay are also linked independent of either a quality control or a stress response (Huch & Nissan 2014). In yeast, inhibition of translation initiation through either 5' cap binding mutants or drug treatment leads to accelerated RNA decay (Schwartz & Parker 1999; Huch & Nissan 2014; Chan et al. 2017). Conversely treatment with cycloheximide, which blocks ribosome elongation, stabilizes RNAs (Beelman & Parker 1994; Huch & Nissan 2014; Chan et al. 2017). These and other data suggest an antagonistic relationship between translation and mRNA degradation.

The link between translational repression and RNA degradation has been intensely debated in the miRNA field (Iwakawa & Tomari 2015; Jonas & Izaurralde 2015). miRNAs are small, non-coding RNAs that bind to the 3' UTR of their target transcripts to inhibit translation and/or induce mRNA destabilization (Fabian & Sonenberg 2012; Jonas & Izaurralde 2015). Ribosome profiling and RNA-Seq experiments demonstrate that miRNAs typically both inhibit translation and destabilize the mRNA of their targets (Eichhorn et al. 2014; Guo et al. 2010). In these studies, the fold change in mRNA levels is larger than the fold change in translational efficiency and the studies conclude that mRNA destabilization is the dominant effect. However, ribosome profiling and RNA-seq in the early zebrafish embryo found that miRNAs induce translational repression without mRNA destabilization (Bazzini et al. 2012). Furthermore, experiments using miRNA reporters to examine the kinetics of miRNA repression suggest that translational repression precedes mRNA destabilization (Djuranovic et al. 2012; Béthune et al.

2012). These studies pose the question of whether translation repression is the primary mode of suppression and mRNA destabilization is a consequence of translation repression or vice versa. Despite extensive research, it is not known whether it is possible to decouple translational repression and mRNA destabilization in a cell where both occur. Additionally, it is unclear whether translational repression of miRNA targets is a prerequisite for their decay.

The RNA-binding protein DDX6 and its yeast homolog DHH1 are DEAD box helicases that localize to P-bodies and stress granules and have been implicated in both translational repression and mRNA destabilization, suggesting that they may link these two processes (Coller & Parker 2005; Presnyak & Coller 2013). Tethering experiments in yeast with decapping or exonuclease mutants suggest that DHH1 can repress translation independent of enhancing decapping (Sweet et al. 2012; Carroll et al. 2011). Tethering experiments in human cells demonstrate that DDX6 also represses translation (Kuzuoğlu-Öztürk et al. 2016). Furthermore, DDX6 binds to components of the decapping complex, potentially enhancing the removal of the 5' cap as another means to reduce translation (Ayache et al. 2015; Tritschler et al. 2009; Nissan et al. 2010). Additionally, through interactions with the CCR4-NOT complex and the decapping complex, DDX6 is involved in miRNA mediated translational repression, but its exact role is not fully understood (Chen et al. 2014; Mathys et al. 2014; Rouya et al. 2014; Chu & Rana 2006).

Here, we sought to understand how mRNA stability changes are linked to translation changes in a mammalian system. It has been suggested that up to 70% of the molecular changes during mouse embryonic stem cell (ESC) differentiation are due to post-transcriptional regulation (Lu et al. 2009). Therefore, we measured and analyzed changes in mRNA stability and translation levels during ESC differentiation. Surprisingly, most changes during this transition are driven at the level of transcription. However, within ESCs there is a wide range of mRNA stabilities. Furthermore, there is a positive correlation between mRNA stability and

translation level within ESCs. We generated DDX6 KO ESCs to understand its role in regulating translation and mRNA stability. The loss of DDX6 results in disruption of ESC morphology and severe proliferation defects. At the molecular level, there was minimal connection between codon usage and stability changes in DDX6 KO ESCs in contrast to data in yeast. However, the loss of DDX6 leads to the translational derepression of miRNA targets without affecting their stability. Furthermore, global translational changes in DDX6 KO ESCs were similar to global translational changes in ESCs that lack all miRNAs demonstrating that the translation repression component of miRNA repression can have a larger role than previously appreciated.

Results

Transcriptional changes drive expression changes during the ESC to EpiLC transition

A previous study suggested that 70% of the molecular changes that occur during early ESC differentiation are due to post-transcriptional events (Lu et al. 2009). In that study, differentiation was induced by expressing a shRNA to Nanog in ESCs grown in LIF. These conditions are associated with a heterogeneous populations of cells. To revisit this question, we first turned to a reporter system and an optimized differentiation protocol that enables the homogenous differentiation of naive ESCs to formative epiblast like cells (EpiLC), which is representative of the transition from the pre to post-implantation epiblast in vivo (Parchem et al. 2014; Krishnakumar et al. 2016) (Figure 9A). Using this system, we characterized the changes in mRNA expression, mRNA stability, and translation that occur during the transition. RNA-Seq showed 1890 genes significantly up-regulated and 1532 genes significantly down-regulated during the ESC to EpiLC transition (Figure 9B, 9E). Known naive markers were down-regulated, while known primed markers were up-regulated during this transition, validating the success of the differentiation (Figure 10A) (Boroviak et al. 2015).

The previous study inferred transcriptional versus post-transcriptional regulation by comparing Pol II binding at the 3' exons of gene bodies, an indirect measure of transcription, with changes in total mRNA levels. In order to directly measure changes in transcription during the ESC to EpiLC transition, we instead used metabolic labeling with 4-thiouridine (4sU) (Dolken et al. 2008; Windhager et al. 2012; Rabani et al. 2011). Nascent transcripts were labeled with a thirty minute 4sU pulse, biotinylated, pulled down with streptavidin, and sequenced (4sU-Seq). Total RNA-Seq was performed in parallel and the ratio of nascent RNA to total RNA was used to calculate relative stabilities for each gene (Rabani et al. 2011). A small subset of genes representing a range of stabilities in the ESC state were validated using an alternative method for measuring stability by blocking transcription with actinomycin D followed by a time course of RT-qPCR measurements (Figure 10C, 10D). The relative stabilities predicted by the two approaches were highly correlated. Given that the 4sU-Seq approach avoids the secondary effects associated with blocking all transcription, we focused on that approach for genome-wide analysis (Lugowski et al. 2017; Bensaude 2011). Surprisingly, the 4sU/total mRNA data showed few significant changes in mRNA stability between the ESC and EpiLC states and most of these changes were small (Figures 9C, 9E). This lack of changes was not because of noise among the replicates, as principal component analysis (PCA) showed strong clustering among the biological replicates (Figures 10E).

The general lack of changes in mRNA stability suggested that transcription is the dominant regulator of the mRNA changes seen during the ESC to EpiLC transition. Indeed, fold changes in total mRNA levels correlated extremely well with fold changes in 4sU labeled nascent transcripts (Spearman's rho 0.88 ; P < $2.22*10^{-16}$) (Figure 9F). Thus, nascent transcription, not mRNA stability, underlies the mRNA changes associated with the ESC to EpiLC transition.

Next, we asked whether changes in translation efficiency play an important role in the ESC to EpiLC transition. To measure translation efficiencies of all genes, we performed ribosome profiling to collect Ribosome Protected Footprints (RPFs) and matched total mRNA (Ingolia et al. 2011). As expected, RPFs showed a strong 3 nucleotide phasing of reads that was not present in the mRNA samples, confirming the quality of the data (Figure 10B). Translational efficiencies were measured as the ratio of RPF/mRNA (Ingolia et al. 2011). Again surprisingly, there were few changes in translational efficiencies between the ESC and EpiLC states (Figures 9D, 9E). PCA confirmed that biological replicates clustered close together suggesting that the overall lack of changes is not due to noise between the replicates (Figures 10F). Therefore, like mRNA stability, there are few changes in translation in early ESC differentiation.

There is a wide range of RNA stabilities which are positively correlated with translation level in ESCs.

Although there are minimal changes in mRNA stability during the ESC to EpiLC transition, there is a wide range of mRNA stabilities within ESCs. For example, between the 25th and 75th percentile of mRNA stability, there is a 3.2 fold difference in stability and between the top and bottom 1% of mRNA stability there is over a 64 fold difference (Figure 11A). To identify features that explain the range of mRNA stabilities observed, we ran a multiple linear regression taking into account the following features that previous studies implicated in affecting mRNA stability: 3' UTR length, 5' UTR length, CDS length, 3' UTR GC content, 5' UTR GC content, CDS GC content, AU rich elements (ARE), miRNA binding sites, number of exons in the transcript, upstream ORFs, and translation level (Sharova et al. 2009; Cheng et al. 2017; Chan et al. 2017). Combined, these features explained 30% of the variation in mRNA stability.

To identify which features had the greatest impact on stability, we analyzed the correlation

between each individual feature and mRNA stability (Figure 11B). 3' UTR length had the largest

negative correlation with mRNA stability (Spearman's rho -0.3; P < 2.22*10^-16) (Figure 11C).

To validate the impact of 3' UTRs on mRNA stability, we used a dual reporter system that

contains a control GFP for normalization and a RFP with a cloned endogenous 3' UTR from 12

representative genes (Figure 11D) (Chaudhury et al. 2014). Flow cytometry analysis of cells

expressing the reporter showed that the RFP/GFP ratio correlated well with the mRNA stability

of the matching endogenous genes measured by 4sU-Seq (Figure 11D). MiRNAs are strong

destabilizers of their RNA targets and primarily bind to their targets' 3' UTR (Fabian &

Sonenberg 2012; Jonas & Izaurralde 2015). Therefore, the presence of additional miRNAs sites

might partially explain why longer 3' UTRs are less stable. In ESCs the embryonic stem

cell-enriched cell cycle (ESCC) family of miRNAs represent a predominant fraction of all

miRNAs in ESCs (Greve et al. 2013; Houbaviy et al. 2003; Marson et al. 2008). As expected,

ESCC miRNA targets were significantly less stable than all genes (P < 2.22*10^-16,

Mann-Whitney test) (Figure 12A). However, a large number of targets were still in the top 50%

of the most stable genes (Figure 12A). Together these data suggest a very large variability in

mRNA stabilities within ESCs, a small part of which can be explained by miRNAs.

Interestingly, analysis of the 4sU-Seq data showed that long non-coding RNAs

(lncRNAs) were significantly less stable than protein coding genes (P < 2.22*10^-16,

Mann-Whitney test) (Figure 11E). This result suggested that there might be a strong connection

between translation and RNA stability in ESCs. To test this hypothesis, we performed polysome

profiling (Heyer & Moore 2016). We isolated a monosome fraction, a low polysome fraction

containing 2-4 ribosomes, and a high polysome fraction containing 4+ ribosomes and performed

RNA-Seq (Figure 12B). Translation levels were defined as the high polysome/monosome ratio.

As expected, protein coding genes had a much higher translation level compared to lncRNAs (P

< 2.22*10^-16, Mann-Whitney test) (Figure 12C). We next compared the polysome profiling data

to the mRNA stability data. There was a highly significant correlation between mRNA stability

and translation levels across all genes, suggesting a direct link between the two (Figure 11F).

Together these data show a wide range of mRNA stabilities in ESC that are negatively

correlated with 3' UTR and positive correlated with translation rates.

DDX6 regulates proliferation and morphology of ESCs.

Recent reports suggest that differential codon usage is a central mechanism in linking

protein translation to mRNA stability (Cheng et al. 2017; Presnyak et al. 2015; Chan et al.

2017). Therefore, we considered the possibility that codon optimality is a driving force in the

wide range of mRNA stabilities. There were small differences in codon usage frequency when

comparing the top and bottom 20% of mRNA stabilities (Figure 12D). In yeast, the protein DHH1

has been shown to link translation, small differences in codon usage, and mRNA stability

(Radhakrishnan et al. 2016). The mammalian homolog of DHH1, DDX6, has been shown to

associate with both the mRNA decapping and deadenylation complex, also consistent with a

potential link between mRNA stability and translation (Chen et al. 2014; Mathys et al. 2014;

Rouya et al. 2014). Therefore, we next asked whether DDX6 may provide a mechanistic link for

the relationship between translation and mRNA stability seen in ESCs.

To investigate the function of DDX6 in ESCs, we produced DDX6 knockout clones using

CRISPR. Sanger sequencing confirmed a single nucleotide insertion in one clone and a large

deletion in a second clone, both of which produce a premature stop (Figure 14A). Western blot

confirmed the absence of DDX6 protein in both clones (Figure 13A). 4sU-Seq and total

RNA-Seq showed that while there was a minimal reduction of nascent *Ddx6* mRNA, there was a

drastic loss of mature *Ddx6* mRNA in the DDX6 KO cells (Figure 13B). This loss likely occurs through nonsense mediated decay and further validates the 4sU-Seq assay for assessing changes in RNA stability.

The loss of DDX6 had little impact on the expression of pluripotency markers (Figure 13C). However, there were striking morphological changes in the cells (Figure 13D). Unlike wild type ESCs which form tight domed colonies, DDX6 KO cells grew in a jagged, dispersed monolayer (Figure 13D). DDX6 localized to discrete punctate in the wild type cells consistent with P-body localization, as previously reported (Figure 13E) (Hubstenberger et al. 2017; Minshall et al. 2009; Ernoult-Lange et al. 2012; Presnyak & Coller 2013). Interestingly, the loss of DDX6 resulted in an abnormal distribution of the P-body marker DCP1, suggesting a role for DDX6 in P-body formation in ESCs (Figure 13F).

DDX6 loss also leads to a reduction in proliferation in self-renewal culture conditions, which was exacerbated when the cells were differentiated (Figure 13G vs 13H). To determine whether the decrease in proliferation was due to a longer cell cycle or increased apoptosis, we took advantage of BAX flox/flox; BAK KO ESCs (Wang et al. 2015). Upon tamoxifen treatment, BAX is knocked out and these cells do not undergo apoptosis. Using CRISPR, we knocked out DDX6 in the BAX flox/flox; BAK KO background. RT-qPCR confirmed the loss of both BAX and DDX6 in these cells following tamoxifen treatment (Figure 14B). DDX6, BAX, BAK triple KO cells again showed a severe reduction in proliferation during differentiation, suggesting an increase in the length of the cell cycle as the major cause (Figure 13I, 13J).

We next asked whether DDX6 KO cells fail to silence the naive pluripotency program or to up-regulate primed markers during differentiation. However, two naive markers of pluripotency (*Nanog* and *Zfp42)* were down-regulated and two markers of primed pluripotency (*Fgf5* and *Otx2*) were up-regulated in the knockout cells to similar levels as their wild type

counterparts (Figure 14C) (Boroviak et al. 2015). Together, these data show that the loss of DDX6 disrupts cell morphology and proliferation.

DDX6 separates miRNA-induced translation repression from RNA degradation

Since yeast DHH1 destabilizes lowly translated transcripts enriched in non-optimal codons, we expected that lowly translated genes might be stabilized in DDX6 KO ESCs (Radhakrishnan et al. 2016). However, there was minimal correlation between mRNA stability changes in DDX6 KO ESCs and wild type translation levels (Figure 15A). The stabilized transcripts were not specifically enriched within the lowly translated transcripts and instead they spanned the spectrum of translation levels. These data suggested that DDX6 does not link mRNA stability with translation across all genes. Next, we defined a set of codons as suboptimal based on their enrichment in unstable genes in wild type ESCs and asked whether they are enriched among genes that are stabilized in DDX6 KO cells (Figure 12D). However, there was no such enrichment (Figure 15B). Further comparing changes in median codon frequency in stable versus unstable transcripts in wild type cells with changes in median codon frequency in stabilized versus unstabilized transcripts in DDX6 KO cells showed no correlation (Figure 15C). Radhakrishnan et al. define codon optimality based on the species specific tRNA adaptation index (sTAI), which is a metric that takes into account tRNA copy number and a tRNA's ability to wobble base pair with different codons (Sabi & Tuller 2014; Radhakrishnan et al. 2016). Transcripts stabilized in DDX6 KO cells were not enriched in transcripts with low sTAI values (Figure 15D). These data suggest that unlike yeast DHH1, the primary function of mammalian DDX6 is not to link codon optimality with transcript stability or such a connection is masked by other factors.

Several aspects of the DDX6 KO phenotype, including the cell morphology changes and growth defects, resemble the phenotype of DGCR8 KO cells (Wang et al. 2007). DGCR8 is essential for miRNA biogenesis and DGCR8 KO ESCs lack all miRNAs (Wang et al. 2007). DDX6 has been implicated as an effector of miRNA activity, but its role is not well understood (Chen et al. 2014; Mathys et al. 2014; Rouya et al. 2014; Chu & Rana 2006). Therefore, we next asked whether DDX6 KO cells have similar downstream molecular consequences as DGCR8 KO cells. To directly compare the two, we performed 4sU-Seq and polysome profiling in DGCR8 KO ESCs and analyzed the data in parallel with the DDX6 KO data.

The embryonic stem cell enriched cell cycle (ESCC) family of miRNAs represent a predominant fraction of all miRNAs in ESCs (Greve et al. 2013; Wang et al. 2008; Melton et al. 2010; Marson et al. 2008; Houbaviy et al. 2003). They share the "AAGUGC" seed sequence and thus have common downstream targets. Furthermore, re-introduction of a single member of the ESCC family of miRNAs can revert DGCR8 KO cells to a molecular phenotype highly similar to wild type ESCs (Gambardella et al. 2017; Wang et al. 2008; Melton et al. 2010). Therefore, we chose to focus on the consequence of DGCR8 loss and DDX6 loss on these targets. As expected, the ESCC targets are stabilized relative to all genes in the DGCR8 KO cells (Figure 16A). However, these same targets showed little change in the DDX6 KO cells (Figure 16B). Therefore, DDX6 does not appear to play a major role in transcript destabilization downstream of miRNAs. Of note, we focus on changes in mRNA stability, rather than changes in mRNA expression, which is a better representation of true targets. While mRNA changes and stability changes of miRNA targets are generally correlated, some predicted miRNA targets change at the mRNA level, but actually have an opposite or minor change in mRNA stability suggesting that these mRNA changes are actually secondary effects (Figure 17A). The loss of DGCR8 also resulted in an increase in translation of ESCC miRNA targets independent of its effect on

stability, consistent with miRNAs both inhibiting translation and destabilizing transcripts (Figure 16C). Surprisingly, the loss of DDX6 had a similar impact as the loss of DGCR8 on the translation of ESCC targets (Figure 16D). Analysis of individual targets showed that DGCR8 KO and DDX6 KO affect the translation of these genes to a similar extent (Figure 16E). Consistent with the idea that DDX6 may be the translational effector of miRNA activity, these findings show that DDX6 separates the impact of miRNAs on translation versus mRNA stability.

Translation changes of miRNA targets are sufficient to rewrite the translatome

Whether translational repression or mRNA destabilization is the predominant effect of miRNAs is controversial as it is difficult to separate the two (Iwakawa & Tomari 2015; Jonas & Izaurralde 2015). Given that the DDX6 KO cells retained mRNA destabilization, while losing translational repression of miRNA targets, we asked how well derepression of translation matches the downstream consequences of losing all miRNAs. Since the DDX6 KO and DGCR8 KO cells have partially overlapping phenotypes, we compared global changes in mRNA stability, mRNA levels, and translation levels. Strikingly, while there was little correlation in changes in mRNA stability, changes in both mRNA and translation levels were well correlated (Figure 18). These data suggest that disruption of the translatome is a major consequence of derepression of translation of miRNA targets. The correlation in mRNA changes is likely partially due to secondary effects of translatome disruption in DDX6 KO and DGCR8 KO cells. These data show that even in the absence of mRNA destabilization, the overall downstream consequences of loss of miRNA induced translation repression resembles the loss of all miRNAs under steady state conditions.

Discussion

In this study we sought to uncover how mRNA stability and translation are regulated within the ESC state and during differentiation. Using RNA-Seq, metabolic labeling (4sU-Seq), ribosome profiling, and polysome profiling, we found that most changes during ESC differentiation are driven at the level of transcription. This find contrasts Lemischka and colleagues finding that post-transcriptional changes represent a large portion of the molecular changes that occur during ESC differentiation (Lu et al. 2009). One possibility is that different culture conditions and differentiation paths account for this discrepancy. Another possibility for this discrepancy is that Lemischka and colleagues focus on comparing nuclear protein levels and mRNA expression, whereas we directly measure translation levels. It is possible that there are significant differences in post-translational regulation such as protein stability or protein localization during ESC differentiation (Liu et al. 2016). Furthermore, mammalian protein half lives tend to be five times more stable than mRNA half lives, suggesting that there may be some lag between changes in mRNA levels and protein levels during differentiation (Schwanhäusser et al. 2011; Jovanovic et al. 2015). While changes in mRNA stability have been observed on short time scales in response to acute stimuli, a recent study comparing changes in protein levels and mRNA levels in dendritic cells in response to LPS stimulation found that transcriptional changes drive most changes in mRNA levels and translation after 12 hours (Hao & Baltimore 2009; Jovanovic et al. 2015; Rabani et al. 2011). Our 3' UTR data and miRNA data suggest that mRNA stability is actively regulated within ESCs. In future experiments, it would be interesting to determine if there are significant changes in mRNA stability in the initial hours as ESCs begin to differentiate before transcriptional changes begin to dominate.

We find a positive correlation between mRNA stability and translation levels in ESCs, similar to what other groups have observed recently in yeast (Heyer & Moore 2016; Presnyak et al. 2015; Chan et al. 2017). The mechanism underlying this connection is still unclear. One

possibility is that ribosomes sterically hinder the degradation machinery from accessing the transcript. In support of this model, RNA-Seq of the 5' end of decapped RNA degradation intermediates showed a three nucleotide periodicity consistent with exonucleases running into the ribosome on a final round of translation (Pelechano et al. 2015). Alternatively, some RNA-binding proteins may sense slowly translating transcripts and accelerate their degradation as recently described for DHH1 (Radhakrishnan et al. 2016). The biological reason for such a mechanism is currently unclear, but could serve as a quality control mechanism. Additionally, some RNA-binding proteins may work to promote both stabilization and high levels of translation of the same transcript to ensure high protein levels of target genes. Likely some combination of all of these mechanisms are at work.

There has been extensive debate about whether miRNAs primarily inhibit translation or induce destabilization of their target transcripts (Iwakawa & Tomari 2015; Jonas & Izaurralde 2015). By analyzing stability changes and translation changes in DGCR8 KO ESCs, which lack all mature miRNAs, we observe that miRNAs both inhibit translation and induce destabilization within ESCs. However, upon loss of DDX6, miRNA targets are derepressed at the translational level without affecting miRNA induced destabilization. It has been suggested that translational repression of miRNA targets is the cause of mRNA destabilization or is at least a prerequisite (Radhakrishnan & Green 2016). However, the DDX6 KO cells demonstrate that RNA destabilization can occur without translational repression in a context where both forms of repression normally occur. Future studies will likely identify factors that can decouple translational repression and mRNA destabilization in the other direction so that miRNA targets are translationally repressed without inducing mRNA destabilization. This situation has been observed in the early zebrafish embryo, but the mechanism underlying the phenomenon remains unclear (Bazzini et al. 2012).

How DDX6 represses translation is not fully understood. Tethering experiments using reporters that do not require 43S scanning for translation demonstrate that DDX6 does not repress scanning (Kuzuoğlu-Öztürk et al. 2016). These experiments suggest that DDX6 suppresses translation initiation. It was recently shown that DDX6 interacts with 4E-T, which competes with eIF4G for binding to the translation initiation factor eIF4E and leads to translational repression (Kamenska et al. 2016; Ozgur et al. 2015). Additionally, mutations in the FDF binding domain of DDX6 prevents interaction with 4E-T and decapping proteins and prevents translational repression of a reporter (Kuzuoğlu-Öztürk et al. 2016). However, depletion of 4E-T only partially alleviates DDX6 mediated translational repression (Kamenska et al. 2014; Kuzuoğlu-Öztürk et al. 2016). Therefore, DDX6 likely interacts with additional unknown factors to inhibit translation initiation. Additional mutagenesis experiments demonstrate that the ATPase domain of DDX6 is required for repression of reporters, but how ATP activity contributes to repression is currently unknown (Mathys et al. 2014).

Surprisingly, we found that while DGCR8 KO and DDX6 KO have similar overall transcriptomes and translatomes, even though the former leads to both stabilization and translational derepression of miRNA targets, while the later only influences translation. Furthermore, DDX6 KO and DGCR8 KO cells both display similar morphology defects and proliferation defects. It has been argued that mRNA changes are the dominant effect of miRNAs, since miRNA induced changes in mRNA levels are often larger than changes in translation efficiency (Guo et al. 2010; Eichhorn et al. 2014). However, our data suggests that while miRNAs often have a significant effect on mRNA stability, their impact on translational alone can recapitulate a large portion of the downstream molecular and phenotypic effects associated with miRNA loss.
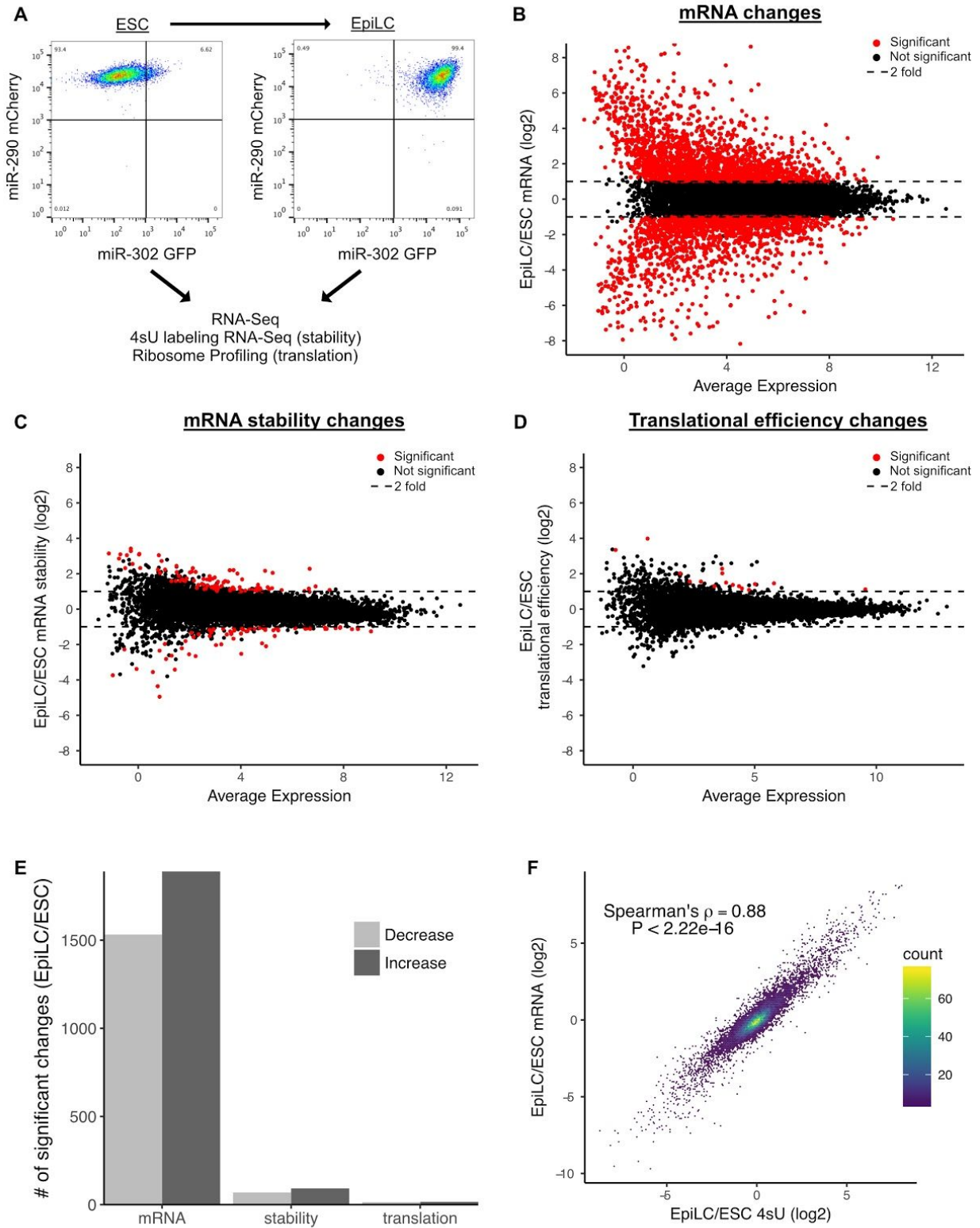
Figure 9 Transcriptional changes drive expression changes during the ESC to EpiLC transition.

A) Flow cytometry of the transition from naive embryonic stem cells (ESCs) (GFP- mCherry+) to primed epiblast-like cells (EpiLCs) (GFP+ mCherry+). B) MA plot of mRNA changes during the ESC to EpiLC transition. Significant changes are shown as red dots (Adjusted P Value < 0.05 and |logFC| > 1) in B-D. Dashed lines indicated a 2 fold change. C) MA plot of mRNA stability changes during the ESC to EpiLC transition. D) MA plot of translational efficiency (TE) changes during the ESC to EpiLC transition. E) The number of significant increases or decreases in mRNA, mRNA stability, and translational efficiency during the ESC to EpiLC transition. F) Correlation between changes in nascent transcription (4sU labeled RNA) and changes in mRNA levels during the ESC to EpiLC transition. P value calculated with correlation significance test.
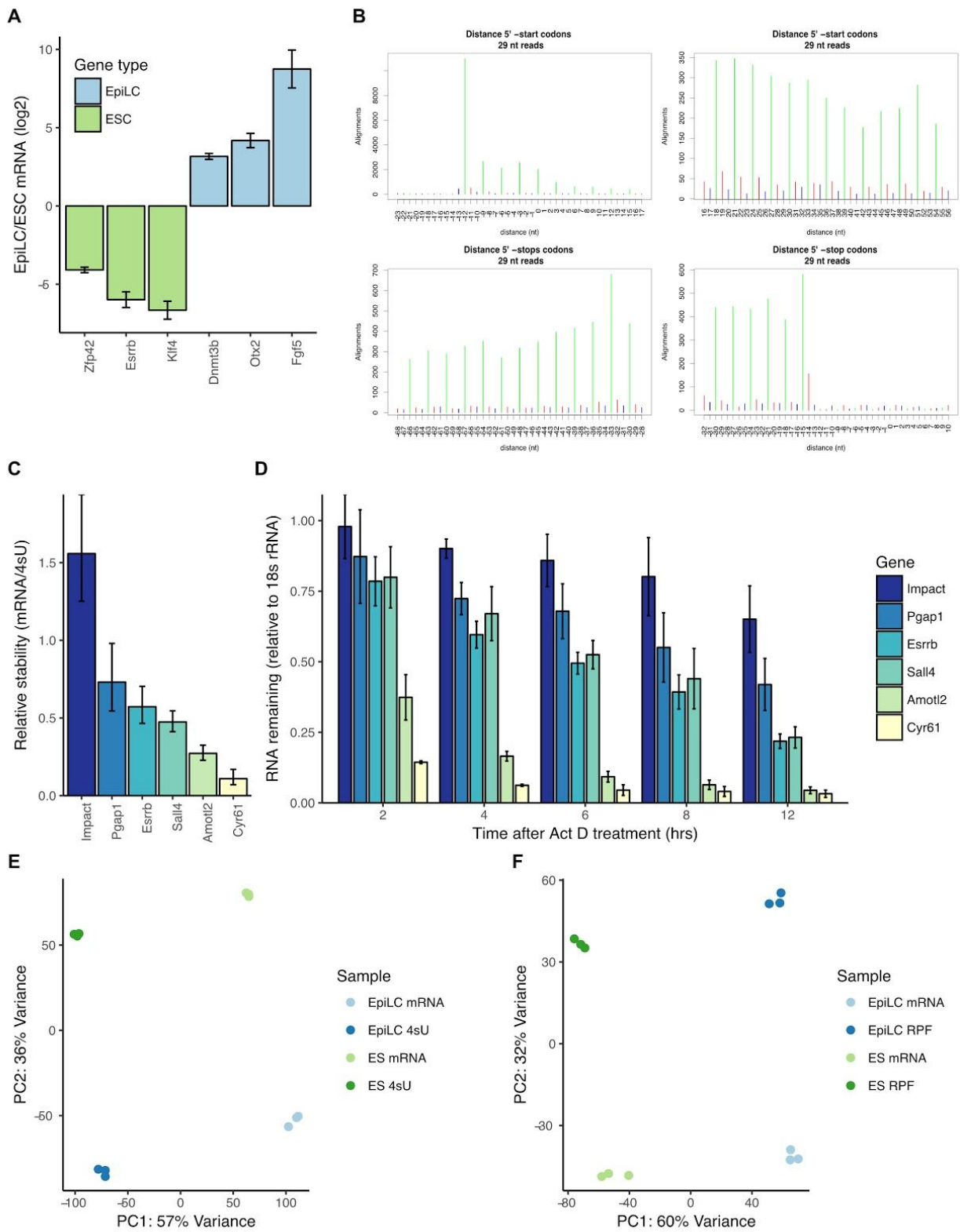
Figure 10 Validation of differentiation, mRNA stability measurements, and ribosome footprinting.

A) Change in expression of key naive and primed genes during the ESC to EpiLC transition based on RNA-Seq. Error bars represent 95% confidence interval. B) Ribosome profiling shows characteristics phasing for ribosome protected footprints. C) Relative mRNA stability of candidate genes based on ratio of mRNA/4sU. Error bars represent 95% confidence interval. D) Validation of 4sU-Seq measured mRNA stabilities with RT-qPCR time course after blocking transcription with Actinomycin D. Values are normalized to 18S rRNA and their 0 hr timepoint. n = 3 for wild type and n = 6 (3 replicates of each DDX6 KO line), error bars are standard deviation. E) PCA plot of ESC and EpiLC RNA-Seq and 4sU-Seq replicates. F) PCA plot of ESC and EpiLC RNA-Seq and ribosome protected footprint (RPF) replicates.
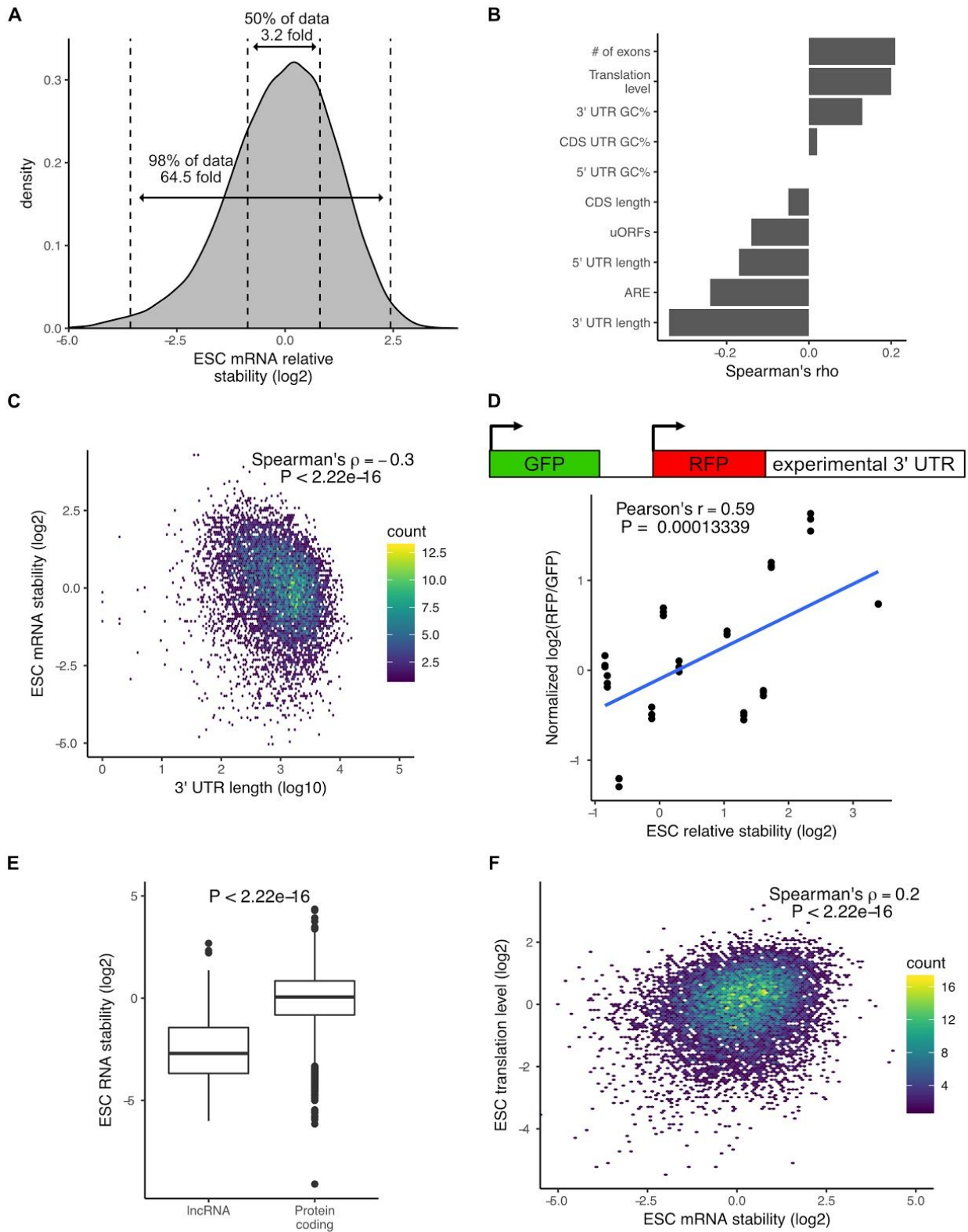
Figure 11 There is a wide range of RNA stabilities which are positively correlated with translation level in ESCs.

A) Distribution mRNA stability ESCs. Dashed lines divide bottom 1%, middle 50%, and top 1% of the data. B) Correlation between different features and mRNA stability in ESCs. C) Comparison between 3' UTR length (log10) and mRNA stability in ESCs. D) (Top) schematic of dual reporter system to test endogenous 3' UTRs. (Bottom) Normalized median RFP/GFP ratios versus mRNA stability for endogenous genes as measured by 4sU-Seq. Clusters of dots indicate an endogenous 3' UTR, individual dots within a cluster represent biological replicates (n = 3). E) RNA stability of long non-coding RNAs (lncRNAs) compared to protein coding RNAs. P value was calculated using the Mann–Whitney test. F) Comparison between mRNA stability and translation level (high polysome / monosome ratio) in ESCs. P value calculated with correlation significance test.
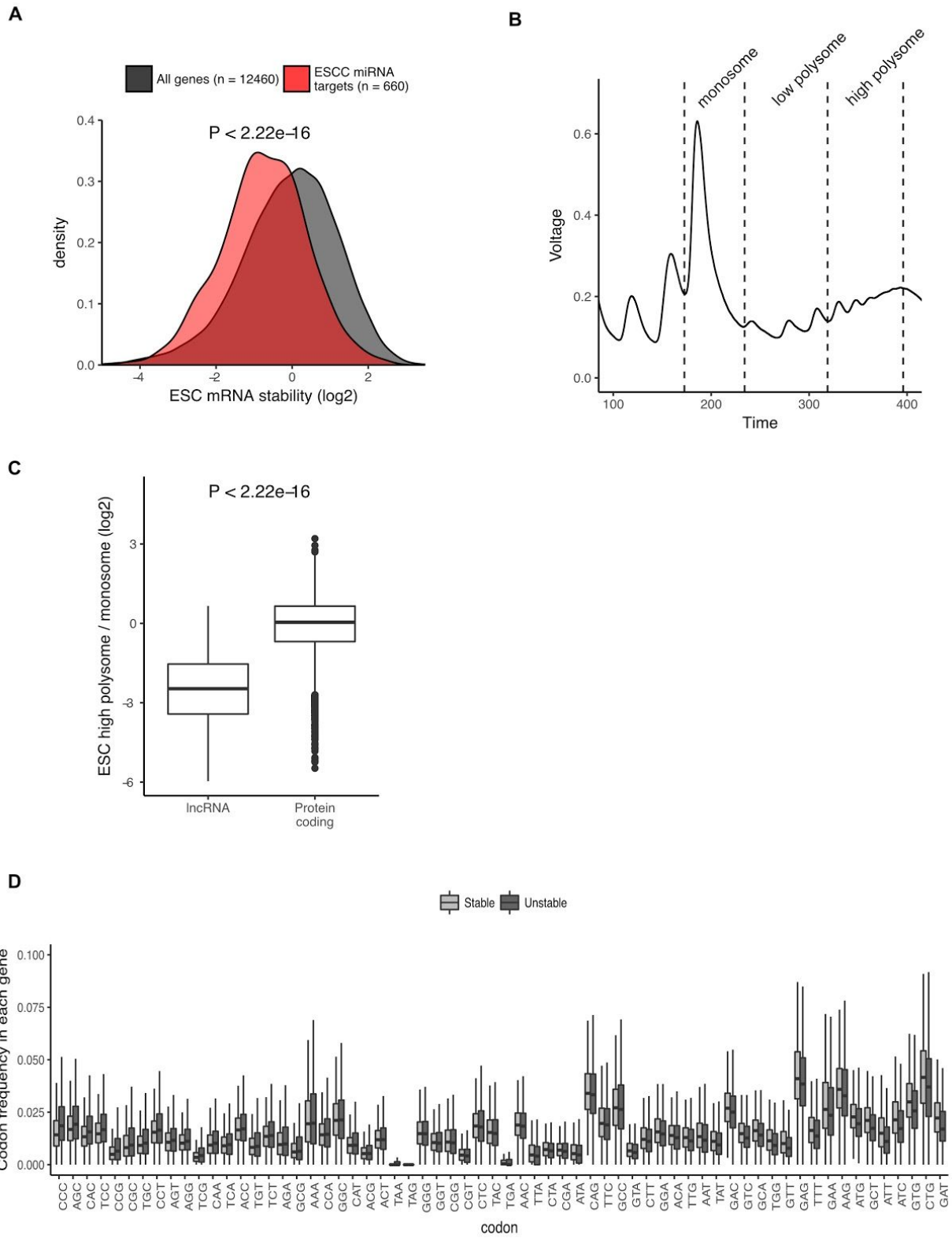
Figure 12 Factors that affect RNA stability in ESCs.

A) mRNA stability of ESCC miRNA targets compared to all mRNAs. P value was calculated using the Mann–Whitney test. B) Polysome trace showing monosome, low polysome, and high polysome fractions collected for RNA-Seq. C) Translation level of long non-coding RNAs (lncRNAs) compared to protein coding RNAs. P value calculated with Mann-Whitney test. D) Boxplots showing the codon usage frequency in the top and bottom 20% of genes in terms of stability. Codons are ordered along the X-axis based on the median codon usage in unstable - median codon usage in stable.
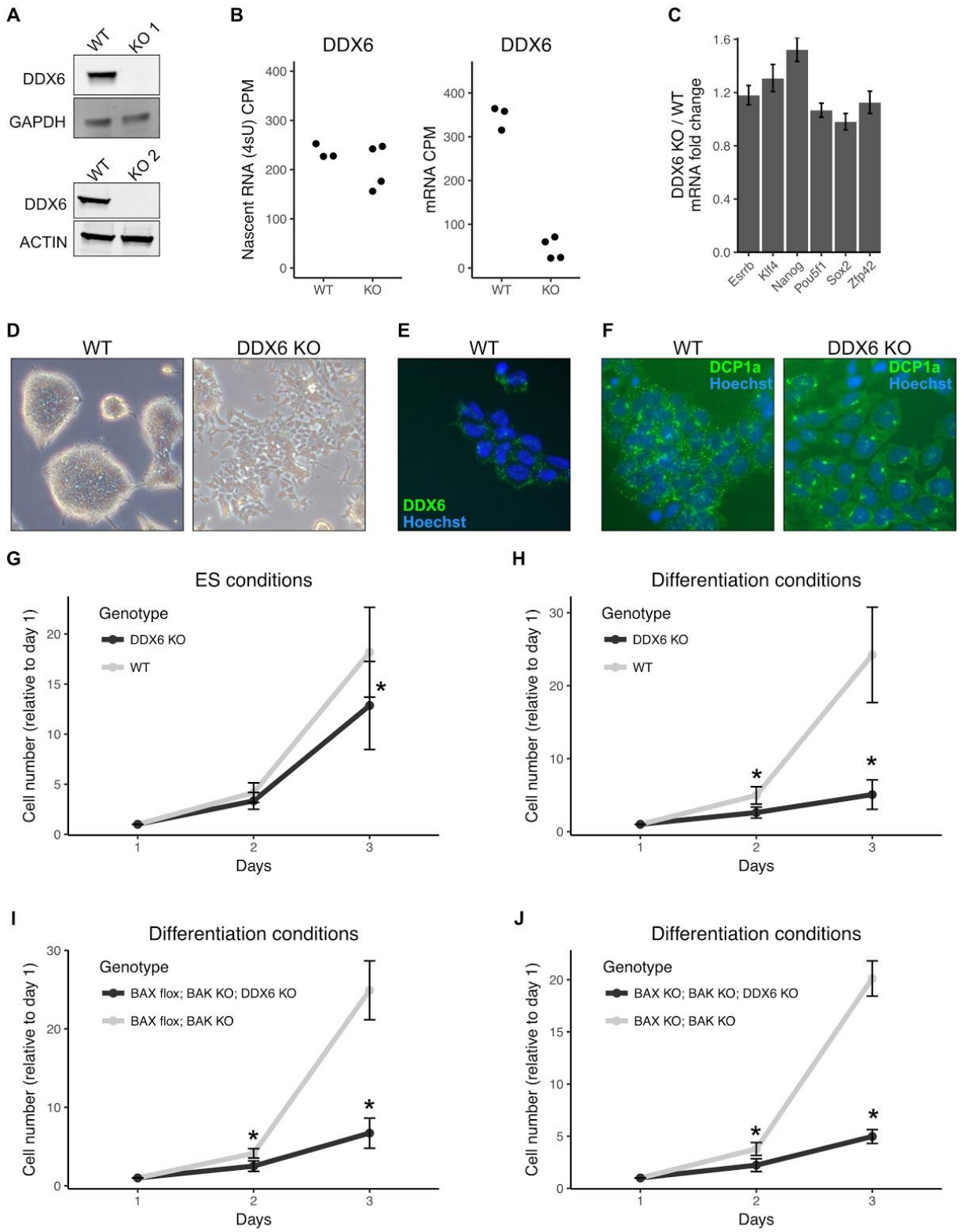
Figure 13 DDX6 regulates proliferation and morphology of ESCs.

A) Western blot of DDX6 in two DDX6 knockout lines. GAPDH and ACTIN were used as loading controls. B) *Ddx6* counts per million (CPM) in nascent RNA (4sU) or mRNA in WT and DDX6 KO cells. C) Expression of pluripotency genes in DDX6 KO ESCs based on RNA-Seq. Error bars represent 95% confidence interval. D) Brightfield images of wild type and DDX6 KO ESCs. Images taken at 20X. E) DDX6 (Green) staining in wild type ESCs. Hoechst is in blue. Images taken at 20X. F) P-body staining against DCP1a (Green) in wild type and DDX6 KO ESCs. Hoechst is in blue. Images taken at 20X. G/H) Growth curves of wild type and DDX6 KO ESCs in ESC maintenance conditions (LIF/2i) (G) or differentiation conditions (removal of LIF/2i) (H). n = 6 for wild type cells, n = 12 (6 replicates of each DDX6 KO line), * indicates P < 0.05 using a t-test, error bars are standard deviation. I) Growth curves of BAX flox/flox; BAK KO or BAX flox/flox; BAK KO;DDX6 KO ESCs during differentiation conditions. J) Growth curves of BAX KO; BAK KO or BAX KO; BAK KO;DDX6 KO ESCs during differentiation conditions. n = 3 for BAX;BAK lines, n = 6 for BAK;BAX;DDX6 KO lines (3 replicates for 2 lines). * indicates P < 0.05 using a t-test, error bars are standard deviation.
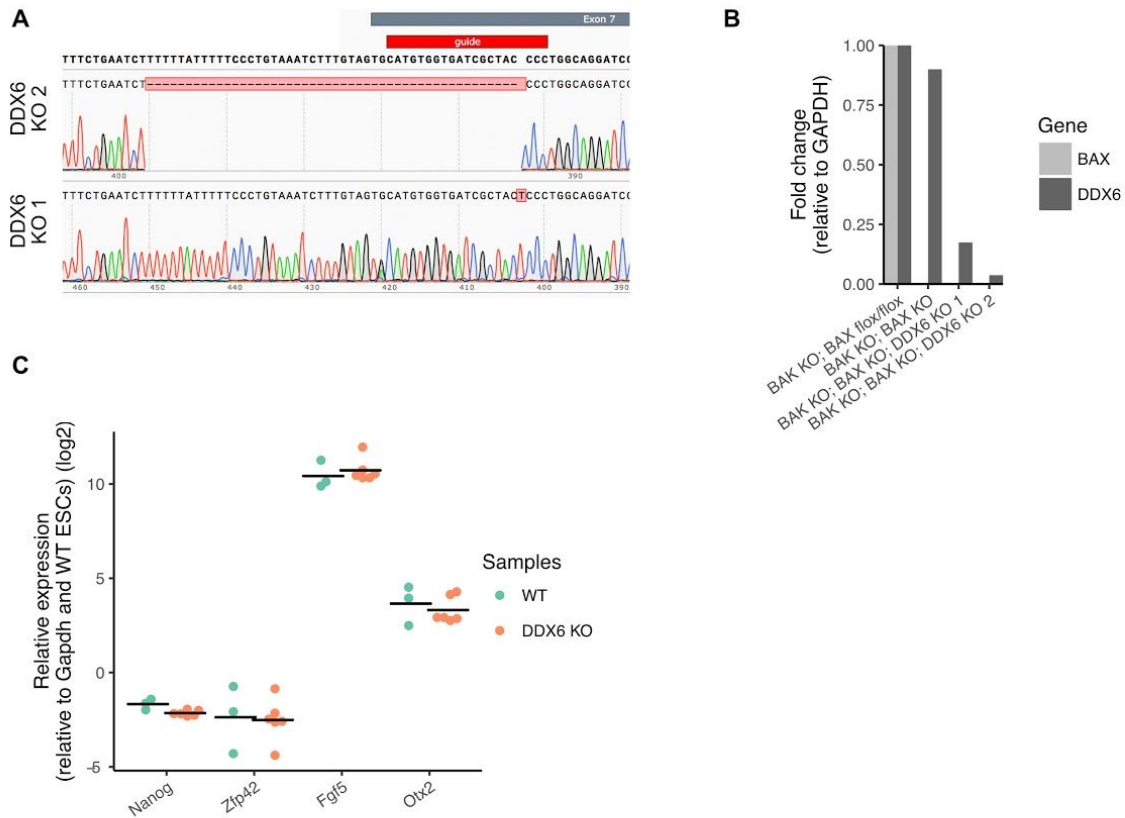
Figure 14 Characterization of DDX6 KO ESCs.

A) Sanger sequencing showing deletion and insertion at the beginning of exon 7 to generate two DDX6 KO clones. B) RT-qPCR validation of BAK KO; BAX flox/flox; DDX6 KO and BAK KO; BAX KO; DDX6 KO lines. C) RT-qPCR for markers of naive pluripotency (*Nanog, Zfp42*) or primed pluripotency (*Fgf5, Otx2*) after differentiation. n = 3 for wild type, n = 6 for DDX6 KO (3 replicates of each DDX6 KO line).
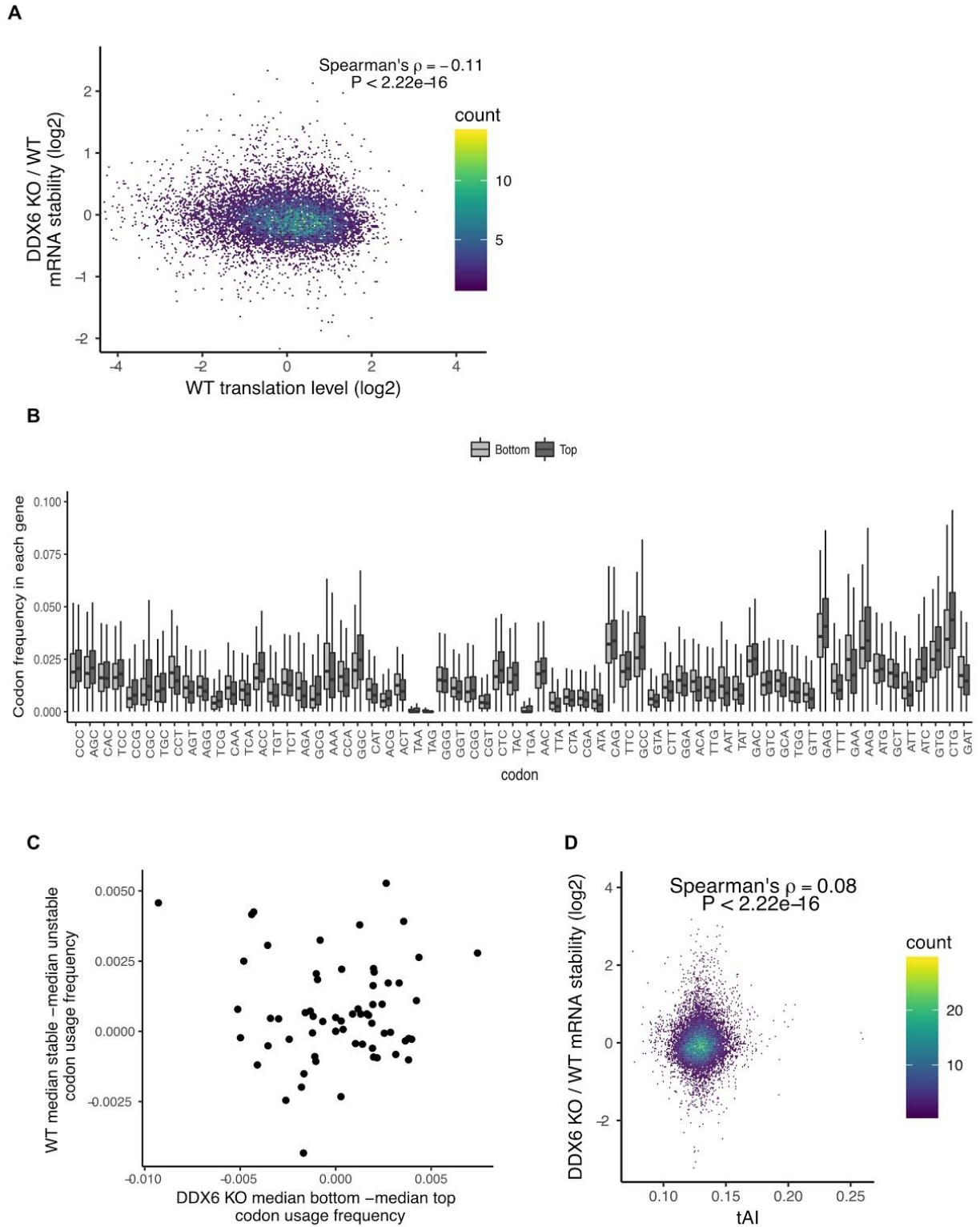
Figure 15 Connection between stability changes and translation.

A) mRNA stability changes in DDX6 KO cells vs wild type translation level. B) Boxplots showing the codon usage frequency in the top and bottom 20% of mRNA stability changes in DDX6 KO for unstable genes as defined in Figure S2D. C) Difference in median codon frequency between stable and unstable transcripts in wild type cells versus difference in median codon frequency between top and bottom DDX6 KO mRNA stability changes. D) mRNA stability changes in DDX6 KO cells vs species specific tRNA adaptation index scores for each gene.
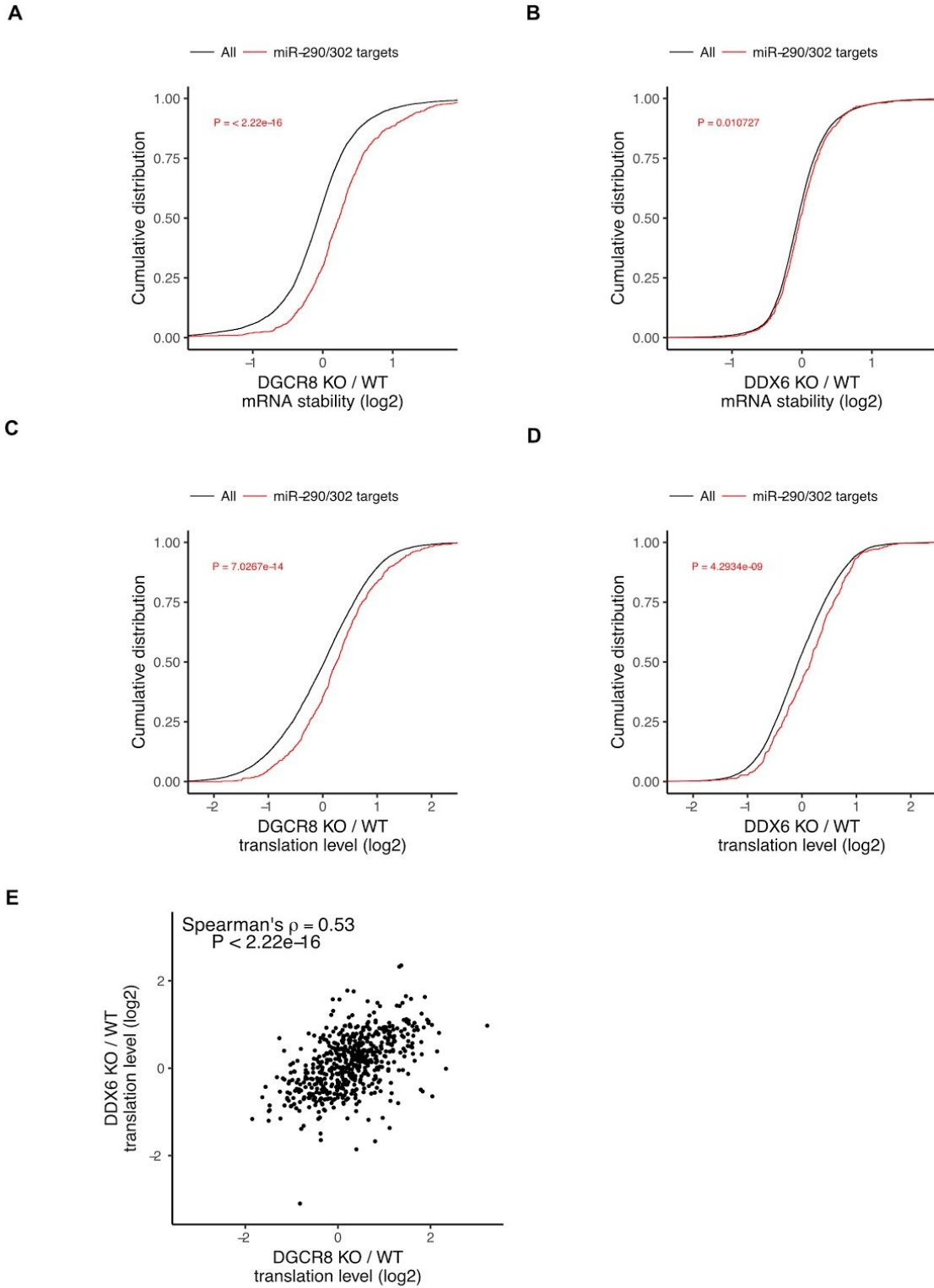
Figure 16 DDX6 separates miRNA-induced translation repression from RNA degradation.

A-D) mRNA stability or translation level changes in ESCC miRNA targets vs all mRNAs. P value calculated with Mann-Whitney test. A/B) mRNA stability changes in DGCR8 KO (A) or DDX6 KO (B). C/D) translation level changes in DGCR8 KO (C) or DDX6 KO (D). Translation level changes of individual ESCC miRNA targets in DGCR8 KO and DDX6 KO ESCs.
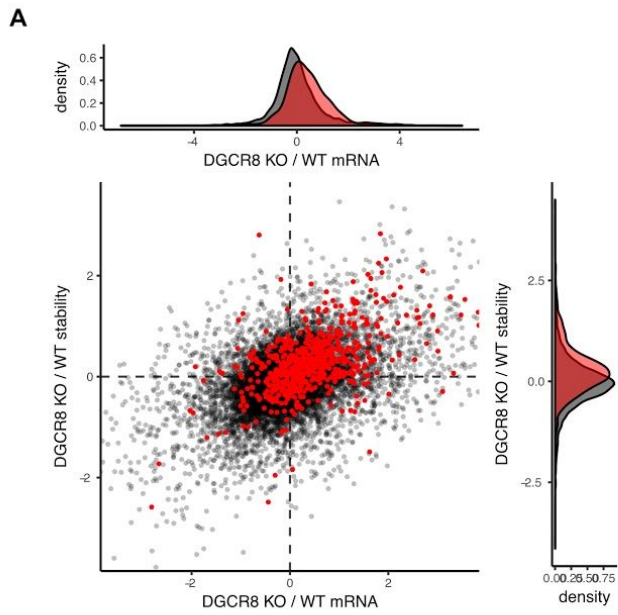
Figure 17 Discrepancy between mRNA changes and stability changes of miRNA targets.
A) mRNA changes vs stability changes in DGCR8 KO cells. ESCC miRNA targets are
highlighted in red.
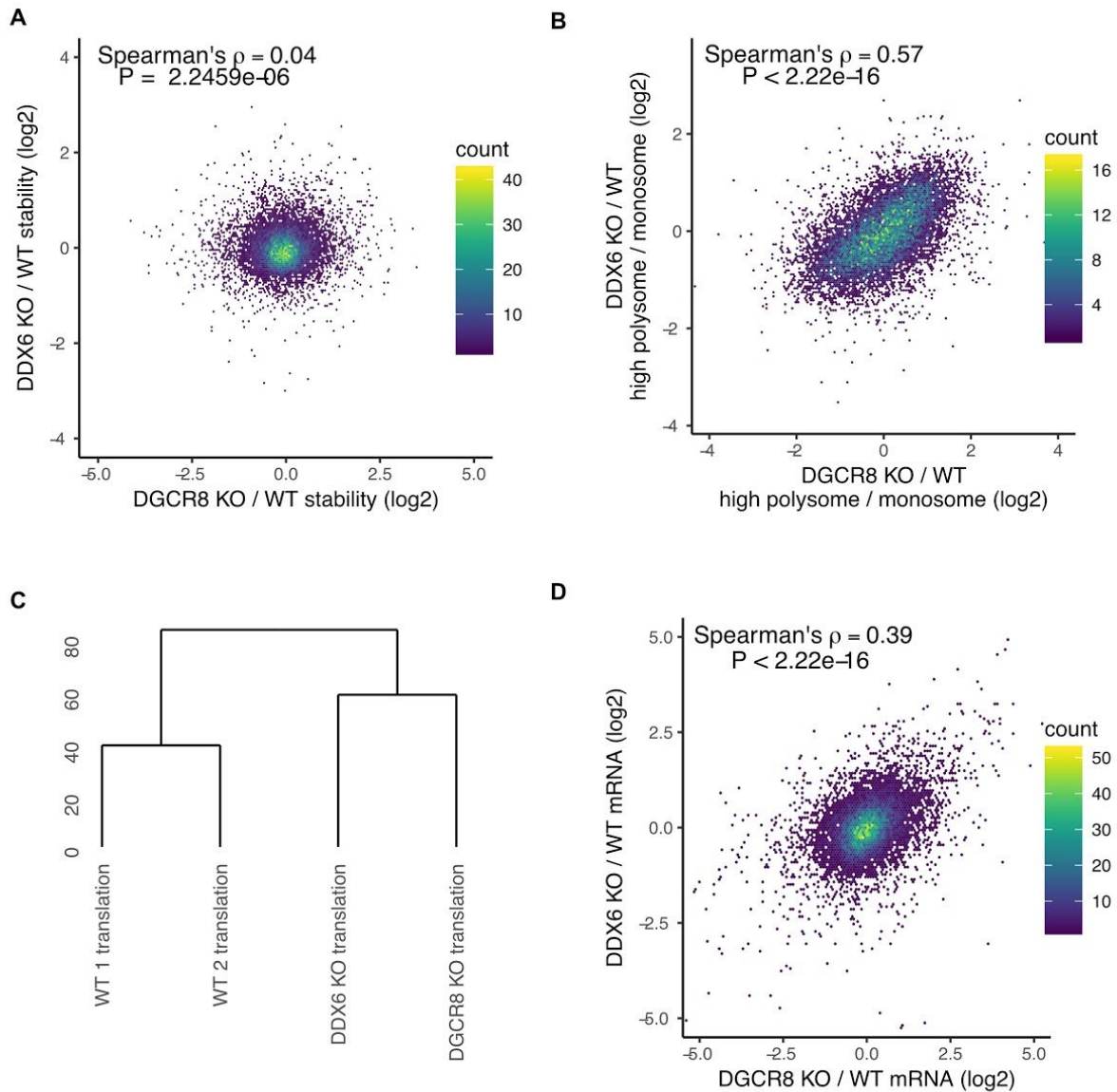
Figure 18 Translation changes of miRNA targets are sufficient to rewrite the translatome.
A) Comparison between mRNA stability changes in DGCR8 KO vs DDX6 KO cells. B)
Comparison between translation level changes in DGCR8 KO vs DDX6 KO cells. C)
Hierarchical clustering of merged DDX6 KO or DGCR8 KO translation level and matched wild
type merged replicates. D) Comparison between mRNA changes in DGCR8 KO vs DDX6 KO
cells. P value calculated with correlation significance test.

Materials and Methods

4sU-Sequencing

Samples were labeled with 500uM 4-thiouridine (4sU) (Sigma) for 30 minutes then extracted

with TRIzol (Invitrogen) and split into two groups. rRNA was depleted from Total RNA using the

Ribo-Zero Gold kit (Illumina). 80 ug of RNA was biotinylated according to the following protocol

Radle et al. (Rädle et al. 2013). Biotinylated 4sU RNA was isolated and washed using M-270

Streptavidin Dynabeads (Invitrogen), eluted with 100mM DTT, and cleaned up with RNeasy

minelute columns (Qiagen).

Libraries were generated with the KAPA Stranded RNA-Seq or Stranded HyperPrep library prep

kit (Kapa) and sequenced with single-end 50 bp reads. Additional rounds of DDX6 KO and

matched WT 4sU samples were sequenced with paired-end reads and counts were merged

with single end reads.

Cell culture and differentiation

ESCs were grown in Knockout DMEM (Invitrogen) supplemented with 15% Fetal Bovine Serum,

LIF and 2i (PD0325901 and CHIR99021). In order to generate EpiLCs, 400,000 ESCs were

plated in a 15cm plate; 24 hours later LIF/2i media was removed, cells were washed with PBS,

and EpiLCs were collected ~ 56 hours later (Krishnakumar et al. 2016). Cells were tested to be

free of mycoplasma.

Quant Seq

QuantSeq 3' end counting was used for polysome profiling samples as well as matched wild

type, DDX6 KO, and DGCR8 KO mRNA samples (Figure 17). RNA was isolated using RNeasy

Micro kits (Qiagen). RNA-Seq libraries were generated using the QuantSeq kit (Lexogen) and sequenced with single-end 50 bp reads.

Ribosome profiling

ESCs and EpiLCs were grown as above. Ribosome profiling libraries were generated using the TruSeq Ribosome Profiling kit (Illumina) and sequenced with single-end 50 bp reads. 3 nucleotide periodicity of ribosome profiling reads was checked using RiboTaper (Calviello et al. 2016).

Polysome Profiling

6 million ESCs were seeded in a 15 cm plate 48 hours prior to collection. Cells were incubated with 100 ug/ml cycloheximide (Sigma) for 2 minutes and then moved to ice. Cells were washed and scraped in PBS with cycloheximide, spun down, and then lysed. Lysate was loaded onto a 10-50% sucrose gradient and centrifuged at 35,000 RPM for 3 hours. Gradients were collected on a gradient station (Biocomp). For each sample, the monosome, low polysome (2-4 ribosomes), and high polysome (4+ ribosomes were collected). RNA was extracted from gradient fractions with TRIzol LS (Invitrogen) and concentrated with the Zymo Clean and Concentrator-5 kit (Zymo) prior to library preparation with the Quant Seq kit (Lexogen).

Western blot

Cells were collected in RIPA buffer with Protease Inhibitor Cocktail (Roche). Protein was run on a 4-15% gel (Bio-Rad) then transferred onto a PVDF membrane. Membranes were blocked with Odyssey blocking buffer, blotted with primary and secondary antibodies, and then imaged on

the Odyssey imaging system (LI-COR). Antibodies: DDX6 1:1000 (A300-460A-T) , GAPDH 1:1000 (SC 25778), ACTIN 1:1000 (A4700).

Actinomycin D RT-qPCR

Cells were treated with 5 ug/ml Actinomycin D. 0, 2, 4, 6, 8, and 12 hours after treatment, RNA was collected in TRIzol (Invitrogen). Reverse transcription was performed with the Maxima first strand synthesis kit (Thermo Scientific). qPCR was then performed with the SensiFAST SYBR Hi-ROX kit (Bioline) on an ABI 7900HT 384-well PCR machine. Each sample was normalized to 18S rRNA and its 0 hour time point.

Differentiation RT-qPCR

Cells were differentiated to an EpiLC state as described above, scaled down to a 6 well dish. Samples were collected in TRIzol (Invitrogen). Reverse transcription was performed with the Maxima first strand synthesis kit (Thermo Scientific). qPCR was then performed with the SensiFAST SYBR Hi-ROX kit (Bioline) on an ABI 7900HT 384-well PCR machine. Each sample was normalized to Gapdh and wild type ESCs in LIF/2i conditions.

BAX/BAK RT-qPCR

Cells were collected in TRIzol (Invitrogen) and RNA was isolated using the Directzol miniprep kit (Zymo). qPCR was then performed with the SensiFAST SYBR Hi-ROX kit (Bioline) on an ABI 7900HT 384-well PCR machine. Each sample was normalized to Gapdh and the parental BAX/BAK cell line.

Cell count

50,000 cells were plated in multiple wells of a 6 well on day 0. On day 1, 2, and 3 cells were trypsinized and counted with a TC20 (Bio-rad). Day 2 and 3 counts were normalized to the day 1 count.

Imaging

Cells were fixed with 4% PFA 10 minutes at room temperature. Cells were blocked with 2% BSA and 1% goat serum in PBST. Cells were incubated with primary antibody for 1 hour at room temperature (Dcp1 abcam (ab47811) antibody 1:800 or DDX6 A300-460A) antibody 1:250). Cells were incubated with goat 488 secondary for 1 hour at room temperature. Cells were then imaged on a Leica inverted fluorescence microscope.

Generation of DDX6 KO ESCs

DDX6 KO lines were generated using the protocol from Ran et al. (Ran et al. 2013). A guide RNA (CATGTGGTGATCGCTACCCC) was cloned into PX458, transfected into ESCs using Fugene 6, and then GFP positive cells were sorted at clonal density. Clones were genotyped with the following primers (Fwd: CATTGCCCAGATTGAAGACA and Rvs: TCCTGACTGGCCTGAAACTT) and verified by western blot. Two different knockout clones were picked and used for all subsequent analysis.

Species specific tRNA adaptation index calculation

For each gene, the CDS region from the Gencode M14 annotation was used. Species specific tRNA adaptation index (sTAI) values for each gene were calculated with stAIcalc (Sabi et al. 2017).

Calculation of codon usage

For each gene, the APPRIS principle isoform was used to calculate codon usage frequency. To analyze differences in codon usage between stable and unstable genes, codon usage frequency was calculated for genes in the top 20% (stable) and bottom 20% (unstable) in terms of wild type mRNA stability. For codon usage frequency for mRNA stability changes in DDX6 KO cells, we first filtered for genes in the bottom 20% of wild type stability as defined above. Within those genes, we took the top 20% (top) and bottom 20% (bottom) of mRNA stability changes in DDX6 KO ESCs and calculated codon usage frequency within each group. For the comparison between codon usage frequency in wild type versus DDX6 KO, we took the median codon usage frequency in stable - the median codon usage frequency in unstable for each codon and compared it to the DDX6 KO median codon usage frequency in the bottom group - median codon usage frequency in the top group, using groups as defined above.

Analysis software

For all samples, adapters were trimmed with Cutadapt version 1.14 with the following options: -m 20. Reads were mapped with STAR version 2.5.3a to the mm10/Gencode M14 genome with the following settings: --outFilterMultimapNmax 1 --outFilterMismatchNoverReadLmax 0.05 --seedSearchStartLmax 25 --winAnchorMultimapNmax 100. Reads were counted with featureCounts version 1.5.3 using the Gencode M14 annotation with rRNA annotations removed with the following settings: -s. Differential expression was carried out with limma version 3.32.10 and R version 3.4.2. For samples with multiple comparisons (e.g. 4sU vs total RNA and KO vs. wild type), a linear model was used for each condition in limma and significant changes in stability or translation are based on the interaction term.

Polysome Profiling Analysis

RNA-Seq from the monosome, low polysome (2-4 ribosomes), and high polysome (4+

ribosomes were collected) fractions was mapped as above. Translation level was defined as the

ratio of the high polysome counts versus the monosome counts. For KO versus wild type

analysis, a linear model was used for each condition in limma and significant changes in

translation are based on the interaction term.

4sU-Seq Analysis

By measuring transcription rate and steady state mRNA levels, it is possible to infer the relative

degradation rate (Rabani et al. 2011). It is assumed that across the population of cells there is

no change in mRNA levels over time for a given state. Therefore, changes mRNA levels can be

modeled by their production rate α and degradation rate β.

$dmRNA/dt = \alpha - \beta[mRNA] \approx 0$

Solving for this equation, degradation rates can be calculated using a production rate (in this

case nascent RNA transcription as measured by 4sU incorporation) and the concentration of

total mRNA in the cell (as measured by total RNA-seq).

$\alpha/[mRNA] \approx \beta$.

Analysis of features regulating RNA stability

For each gene with multiple isoforms, the APPRIS principle isoform was used. APPRIS data

were downloaded on 10/30/2017. Log10 Feature lengths, GC %, and number of exons were

calculated in R version 3.4.2. Upstream ORFs were defined as the number of ATG sequences

in the 5' UTR. AU rich elements were defined as the number of UAUUUAU sequences in the 3'

UTR. miRNA sites were defined as below. Each of these features were used in a multiple linear

regression using the lm function in R version 3.4.2. Additionally, the Spearman correlation was calculated between each feature and mRNA stability.

3' UTR analysis

For each gene, the APPRIS principle isoform was used to calculate log10 (3' UTR length). Log10(3' UTR length) was then compared to log2 relative mRNA stability.

3' UTR reporters

Endogenous 3' UTRs from the following genes were amplified from ESC cDNA: ENSMUSG00000021583, ENSMUSG00000029580, ENSMUSG00000043716, ENSMUSG00000010342, ENSMUSG00000021665, ENSMUSG00000024406, ENSMUSG00000052911, ENSMUSG00000058056, ENSMUSG00000020105, ENSMUSG00000026003, ENSMUSG00000020038, ENSMUSG00000025521, ENSMUSG00000031503. Genes were cloned into the pBUTR (piggyBac-based 3′ UnTranslated Region reporter) using gateway cloning as outlined in Chaudhury et al (Chaudhury et al. 2014). Reporters were transfected into ESCs using Fugene 6 (Promega). Cells were treated with Genenticin to enrich for transfected cells. Cells were analyzed on an LSRII (BD). RFP+/GFP+ cells were gated in FlowJo and median RFP/GFP ratios were calculated. RFP/GFP ratios were standardized between days to accounts for differences in laser power.

microRNA targets

Conserved microRNA targets were downloaded from Targetscan mouse release 7.1. This list was filtered for genes that are targeted by the miR-291-3p/294-3p/295-3p/302-3p family yielding 765 target genes.

Primers

	Forward	Reverse
Gapdh	AGGTCGGTGTGAACGGATTTG	TGTAGACCATGTAGTTGAGGTCA
Nanog	AACCAAAGGATGAAGTGCAAGCGG	TCCAAGTTGGGTTGGTCCAAGTCT
Zfp42	CTCCTGCACACAGAAGAAAGC	CACTGATCCGCAAACACC
Fgf5	CCTTGCGACCCAGGAGCTTA	CCGTCTGTGGTTTCTGTTGAGG
Otx2	CAACTTGCCAGAATCCAGGG	GGCCTCACTTTGTTCTGACC
Bak	gctgacatgtttgctgatgg	gatcagctcgggcactttag
Ddx6 qPCR	ACTATACTCCGCTACTTTCCCTC	TGGCGCTCCGTTACATATG
18S	GTGGAGCGATTTGTCTGGTT	CGCTGAGCCAGTCAGTGTAG
MycN	AGTGTGTCTGTTCCAGCTACTG	TTCATCTTCCTCCTCGTCATCC
Pgap1	AGTACCCCGAGTACCAGAAAAT	TCGAACTTGCTTATAGCTTCCAG
Impact	GTGAAGAAATCGAAGCAATGGC	GGTACTCACTTGGCAACATCA
Cyr61	AACGAGGACTGCAGCAAAAC	TTCTGACTGAGCTCTGCAGATC
Amotl2	AGGGACAATGAGCGATTGCAG	CCTCACGCTTGGAAGAGGT
Ddx6 Genotyping	CATTGCCCAGATTGAAGACA	TCCTGACTGGCCTGAAACTT

Chapter 4 - Conclusions and future remarks

The projects presented in this thesis provide novel insights into the broad questions of how miRNA activity is globally regulated and how the multiple downstream effects of miRNA binding are individually regulated. In the first project, we examined why miRNA activity is lost in maturing oocytes. We showed that the loss of miRNA activity is partially due to limiting levels of miRNA-AGO. Injection of exogenous miRNA-AGO rescues the translational repression of a reporter, but has a minimal impact on either the reporter or endogenous transcript levels. In the second project, we examined the connection between translation and mRNA stability in mouse embryonic stem cells. Focusing on miRNA targets, we found that miRNA targets are both translationally repressed and destabilized at the mRNA level. The loss of all miRNAs in DGCR8 KO ESCs leads to increased translation and stability of miRNA targets. However, the loss of the RNA-binding protein DDX6 decouples these two forms of repression. The loss of DDX6 leads to increased translation of miRNA targets, without affecting their stability. The results of these studies raise many interesting questions and future directions, which are discussed below.

Why is miRNA activity silenced in oocytes?

We showed that suppression of miRNA activity during oocyte maturation is evolutionarily conserved. Furthermore, we showed that although we could re-activate miRNA repression of a reporter, endogenous transcripts were not affected. This finding suggests that there are multiple redundant mechanisms that protect endogenous transcripts from miRNA activity. These two findings suggest that it is critical that miRNA activity is silenced in maturing oocytes. The suppression of miRNA activity might enable the expression of factors that are critical for reprogramming a somatic oocyte to a totipotent zygote. It has been speculated that zygotic activation of the miR-290 family plays a role in establishing pluripotency in the early embryo

(Svoboda & Flemr 2010; Giraldez 2010). However, the let-7 family, which antagonizes the miR-290 family, is abundantly expressed in the oocyte (Svoboda & Flemr 2010; Melton et al. 2010). Suppression of miRNA activity in the oocyte may be necessary to allow the miR-290 family to take over for the let-7 family in the early embryo. Alternatively, the importance of redundant mechanisms to prevent miRNA activity may reflect the inability to replace transcripts once degraded as Pol II driven expression is repressed during this critical phase of mammalian development. In future work, if it is possible to re-activate miRNA induced destabilization of endogenous mRNA targets in the oocyte, it will be interesting to examine how reprogramming and early embryogenesis is affected.

How are endogenous transcripts protected?

We showed that the introduction of exogenous AGO2 and miRNA leads to the translational repression of a reporter, but microarray profiling showed minimal changes in the expression of endogenous transcripts. It is possible that the translation of endogenous transcripts was changed, but it seems unlikely that the suppression of translation of the many miR-15 targets expressed in the oocytes would not, at least indirectly, result in observable changes in mRNA levels. We also found that several effectors of miRNA activity are lowly expressed in the oocyte. Most notably, several proteins involved in exonucleolytic decay including XRN1, the primary 5' to 3' exonuclease downstream of miRNA activity, are also lowly expressed in oocytes. Furthermore, components of the deadenylation and decapping complexes are lowly expressed and minimally active in GV oocytes (Ma et al. 2015; Ma et al. 2013). Additionally, RNA-binding proteins in the oocyte may antagonize miRNA activity. Deadenylation of mRNA targets is a major step in miRNA induced degradation (Jonas & Izaurralde 2015). However, the presence of cytoplasmic polyadenylation in oocytes could

antagonize miRNA induced deadenylation (Racki & Richter 2006). Furthermore, important

oocyte RNA-binding proteins such as Pumilio and Dead end 1 have been shown to block the

binding and activity of specific miRNAs in other contexts (Kedde et al. 2010). These and other

RNA-binding proteins might broadly antagonize miRNA activity in the oocyte. In future

experiments, it would be interesting to either overexpress or knockdown some of these factors

along with introducing exogenous miRNA-AGO, to determine if it is possible to destabilize

endogenous targets.

What other mechanisms globally regulate miRNA activity?

Although we showed that AGO2 is lowly expressed in the oocyte, there is enough AGO2

for siRNA activity. Independent knockout of DGCR8 and AGO2 in oocytes demonstrated that

the loss of miRNAs had no effect, but the loss of AGO2 causes the oocytes to arrest (Kaneda et

al. 2009; Suh et al. 2010). This result demonstrates that some functional AGO2 exists in the

oocyte. The low levels of full length AGO2 may be enough for the observed siRNA function, but

not miRNA function. Indeed, siRNA slicing is a much more efficient process than miRNA

directed mRNA destabilization and thus likely to require significantly less AGO2 (Ebert et al.

2007). However, it is also possible that either a repressor protein or post-translational

modification to AGO prevents miRNA activity, while not affecting AGO slicer activity. It was

recently shown that a cycle of phosphorylation and dephosphorylation of AGO is essential for

miRNA activity (Golden et al. 2017). We analyzed published expression profiling data to identify

whether the expression of the kinase and phosphatase identified by Golden et al. changed

during oocyte maturation, but the results were inconsistent between data sets. Although

technically challenge, it would be interesting for future studies to identify unique AGO interactors

and post-translational modifications in the oocyte.

How do developmental cues affect post-transcriptional regulation?

Post-transcriptional mechanisms enable a cell to rapidly change protein levels in response to external cues (Liu et al. 2016). Considering that the median half-life of mammalian mRNAs is at least several hours, active degradation allows the clearance of unwanted messages much faster than transcriptional shut off alone (Schwanhäusser et al. 2011). Active regulation of translation coupled with active regulation of mRNA levels, allow the cell to change protein levels without the delay of transcriptional regulation alone. Post-translational modifications can complement post-transcriptional changes to further stabilize or degrade select proteins without the delay of transcriptional regulation. Beyer et al. found that in yeast a number of transcription factors are subject to what they term "translation on demand", in which the mRNA in constitutively present, but not translated until some external cue (Beyer et al. 2004; Liu et al. 2016). One example of this is the transcription factor GCN4, which is constitutively expressed, but only translated under amino acid starvation allowing for rapid production of the protein (Hinnebusch & Natarajan 2002). A recent study analyzed changes in protein levels and mRNA levels in mouse dendritic cells in response to LPS stimulation. While most protein changes were driven by mRNA changes, they found several key transcription factors were translationally upregulated supporting the concept of translation on demand (Jovanovic et al. 2015). The authors further found increased degradation of certain proteins in response to LPS (Jovanovic et al. 2015). It will be interesting to determine if increased degradation of specific proteins or mRNAs is a common feature required in other cell state changes.

It will be interesting for future studies to investigate mRNA stability changes and translation changes in the first several hours of ESC differentiation. ESCs must balance self-renewing in a pluripotent state with the ability to differentiate in response to external cues. The self-renewal network must be robust to not induce precocious differentiation due to noise,

but flexible enough to differentiate in response to the correct cues. Therefore, it is likely that post-transcriptional regulation plays a role in actively clearing key components of the pluripotent network to allow the cells to differentiate. It is also likely that key differentiation regulators are rapidly induced to commit the cells to differentiation.

Does codon usage regulate translation and mRNA stability?

Presnyak et al. recently claimed that codon optimality is the major determinant of mRNA stability in yeast (Presnyak et al. 2015). Follow up work showed that DHH1 senses slowly translating transcripts enriched in non-optimal codons and leads to higher levels of mRNA degradation (Radhakrishnan et al. 2016). However, we found that there was minimal correlation between mRNA stabilized in DDX6 KO ESCs and translation level in wild type ESCs. We further analyzed mRNA stability changes with regard to the species specific tRNA adaptation index (sTAI) as used by Radhakishnan et al. to define optimal and non-optimal codons (Sabi & Tuller 2014; Radhakrishnan et al. 2016). However, we again saw no connection between mRNA stability changes in DDX6 KO ESCs and transcripts with a low sTAI. There are several possibilities for this discrepancy.

First, there is only a 63% similarity between the yeast DHH1 and mammalian DDX6 proteins, so their function in terms of sensing codon optimality may have diverged (Presnyak & Coller 2013). Second, codon optimality is driven in part through tRNA abundance, which is cell type specific in mammals and can alter translation and mRNA stability in a cell type specific manner (Gingold et al. 2014; Goodarzi et al. 2016). tRNA abundance data does not exist for ESCs and quantitative sequencing protocols are still being developed, making it difficult to definitively assign transcripts as enriched in optimal or non-optimal codons in ESCs. Third, mammalian median 3' UTR length is ten times longer than yeast 3' UTR length, creating

additional regulatory sites for post-transcriptional regulation (Mayr 2017). RNA-binding proteins

and miRNAs significantly regulate mRNA stability in ESCs, reducing the impact that codon

usage might have on mRNA stability compare to yeast. Fourth, Subtelny et al. found that

poly(A) tail length is coupled to translational efficiency in early zebrafish and frog embryos, but

not in yeast or somatic cells (Subtelny et al. 2014). It is possible that similar mechanisms exist in

ESCs, reducing the impact that codon usage has on translation levels. Lastly, a correlation

between mRNA stability and both general translation levels and transcript abundance also

exists (Chan et al. 2017). It is likely that high translation levels, transcript abundance, and codon

optimality have co-evolved making it difficult to disentangle the contribution of any individual

feature to transcript stability.

How do RNA-binding proteins regulate mRNA stability and translation?

We found that 3' UTR length is the feature that is most correlated with mRNA stability in

ESCs. Furthermore, we cloned a number of endogenous 3' UTRs into a dual reporter system.

The 3' UTRs were cloned downstream of RFP and the construct contained a control GFP driven

by an independent promoter (Figure 11D). When this construct was introduced into ESCs, the

ratio of RFP/GFP was significantly correlated with endogenous mRNA stability (Figure 11D).

This result suggests that these 3' UTRs can significantly regulate mRNA abundance and/or

translation in ESCs. These 3' UTRs are likely bound by a number of RNA-binding proteins that

influence the stability and translation level of the transcript (Glisovic et al. 2008; Ye & Blelloch

2014; Van Nostrand et al. 2017). It is interesting to note that mammalian median 3' UTR length

is ten times longer than yeast 3' UTR length (Mayr 2017). Furthermore, there are similar

numbers of RNA-binding proteins as there are transcription factors (Gerstberger et al. 2014).

However, compared to transcription factors much less is known about RNA-binding proteins'

function and targets. One issue is that RNA-binding proteins display pleiotropic and redundant roles (Turner & Díaz-Muñoz 2018). The other issue is that most RNA-binding proteins do not have known targets or a known binding motif.

The development and improvement of UV crosslinking and immunoprecipitation (CLIP) protocols over the past 15 years has enabled the genome wide detection of RNA-binding protein targets (Lee & Ule 2018). Recently, the targets and binding sites for several hundred RNA-binding proteins was described (Van Nostrand et al. 2016). ENCODE plans to identify the targets of most human RNA-binding proteins (Van Nostrand et al. 2017). In addition to identifying targets and binding motifs, these studies will provide insights into the functions of individual RNA-binding proteins and identify which RNA-binding proteins co-regulate the same targets. In parallel, recent advances have enabled the high throughput characterization of RNA-binding protein binding motifs *in vitro* (Lambert et al. 2014; Buenrostro et al. 2014). ENCODE is also applying these techniques to map the binding preferences of most RNA-binding proteins (Dominguez et al. 2017). Together, this work will greatly facilitate future studies to elucidate the roles of RNA-binding proteins in regulating both mRNA stability and translation. Furthermore, such studies will continue to elucidate the importance of post-transcriptional regulation in controlling mRNA and protein levels in both steady state and in differentiation conditions.

References

Abe, K.-I. et al., 2010. Global gene silencing is caused by the dissociation of RNA polymerase II from DNA in mouse oocytes. *The Journal of reproduction and development*, 56(5), pp.502–507.

Adivarahan, S., Rahman, S. & Zenklusen, D., 2017. Spatial organization of single mRNPs at different stages of the gene expression pathway. Available at: http://dx.doi.org/10.1101/237008.

Alemán, L.M., Doench, J. & Sharp, P.A., 2007. Comparison of siRNA-induced off-target RNA and protein effects. *RNA* , 13(3), pp.385–395.

Arribas-Layton, M. et al., 2013. Structural and functional control of the eukaryotic mRNA decapping machinery. *Biochimica et biophysica acta*, 1829(6-7), pp.580–589.

Ayache, J. et al., 2015. P-body assembly requires DDX6 repression complexes rather than decay or Ataxin2/2L complexes. *Molecular biology of the cell*, 26(14), pp.2579–2595.

Babiarz & Blelloch, 2009. Small RNAs – their biogenesis, regulation and function in embryonic stem cells. *StemBook*. Available at: http://dx.doi.org/10.3824/stembook.1.47.1.

Babiarz, J.E. et al., 2008. Mouse ES cells express endogenous shRNAs, siRNAs, and other Microprocessor-independent, Dicer-dependent small RNAs. *Genes & development*, 22(20), pp.2773–2785.

Bartel, D.P., 2009. MicroRNAs: Target Recognition and Regulatory Functions. *Cell*, 136(2), pp.215–233.

Bazzini, A.A., Lee, M.T. & Giraldez, A.J., 2012. Ribosome profiling shows that miR-430 reduces translation before causing mRNA decay in zebrafish. *Science*, 336(6078), pp.233–237.

Beelman, C.A. & Parker, R., 1994. Differential effects of translational inhibition in cis and in trans on the decay of the unstable yeast MFA2 mRNA. *The Journal of biological chemistry*, 269(13), pp.9687–9692.

Bensaude, O., 2011. Inhibiting eukaryotic transcription. Which compound to choose? How to evaluate its activity? *Transcription*, 2(3), pp.103–108.

Bernstein, E. et al., 2003. Dicer is essential for mouse development. *Nature genetics*, 35(3), pp.215–217.

Béthune, J., Artus-Revel, C.G. & Filipowicz, W., 2012. Kinetic analysis reveals successive steps leading to miRNA-mediated silencing in mammalian cells. *EMBO reports*, 13(8), pp.716–723.

Beyer, A. et al., 2004. Post-transcriptional expression regulation in the yeast Saccharomyces cerevisiae on a genomic scale. *Molecular & cellular proteomics: MCP*, 3(11), pp.1083–1092.

Boroviak, T. et al., 2015. Lineage-Specific Profiling Delineates the Emergence and Progression

of Naive Pluripotency in Mammalian Embryogenesis. *Developmental cell*, 35(3), pp.366–382.

Buenrostro, J.D. et al., 2014. Quantitative analysis of RNA-protein interactions on a massively parallel array reveals biophysical and evolutionary landscapes. *Nature biotechnology*, 32(6), pp.562–568.

Calviello, L. et al., 2016. Detecting actively translated open reading frames in ribosome profiling data. *Nature methods*, 13(2), pp.165–170.

Cantone, I. & Fisher, A.G., 2013. Epigenetic programming and reprogramming during development. *Nature structural & molecular biology*, 20(3), pp.282–289.

Carroll, J.S., Munchel, S.E. & Weis, K., 2011. The DExD/H box ATPase Dhh1 functions in translational repression, mRNA decay, and processing body dynamics. *The Journal of cell biology*, 194(4), pp.527–537.

Chang, H. et al., 2014. TAIL-seq: Genome-wide Determination of Poly(A) Tail Length and 3′ End Modifications. *Molecular cell*, 53(6), pp.1044–1052.

Chan, L.Y. et al., 2017. Non-invasive measurement of mRNA decay reveals translation initiation as the major determinant of mRNA stability. Available at: http://dx.doi.org/10.1101/214775.

Chaudhury, A. et al., 2014. A piggyBac-based reporter system for scalable in vitro and in vivo analysis of 3′ untranslated region-mediated gene regulation. *Nucleic acids research*, 42(10), pp.e86–e86.

Cheng, J. et al., 2017. -regulatory elements explain most of the mRNA stability variation across genes in yeast. *RNA* , 23(11), pp.1648–1659.

Chen, Q. & Hu, G., 2017. Post-transcriptional regulation of the pluripotent state. *Current opinion in genetics & development*, 46, pp.15–23.

Chen, Y. et al., 2014. A DDX6-CNOT1 Complex and W-Binding Pockets in CNOT9 Reveal Direct Links between miRNA Target Recognition and Silencing. *Molecular cell*, 54(5), pp.737–750.

Chiang, H.R. et al., 2010. Mammalian microRNAs: experimental evaluation of novel and previously annotated genes. *Genes & development*, 24(10), pp.992–1009.

Chong, M.M.W. et al., 2010. Canonical and alternate functions of the microRNA biogenesis machinery. *Genes & development*, 24(17), pp.1951–1960.

Christie, M. et al., 2013. Structure of the PAN3 pseudokinase reveals the basis for interactions with the PAN2 deadenylase and the GW182 proteins. *Molecular cell*, 51(3), pp.360–373.

Chu, C.-Y. & Rana, T.M., 2006. Translation repression in human cells by microRNA-induced gene silencing requires RCK/p54. *PLoS biology*, 4(7), p.e210.

Coller, J. & Parker, R., 2005. General translational repression by activators of mRNA decapping.

Cell, 122(6), pp.875–886.

Djuranovic, S., Nahvi, A. & Green, R., 2012. miRNA-mediated gene silencing by translational repression followed by mRNA deadenylation and decay. *Science*, 336(6078), pp.237–240.

Dobin, A. et al., 2013. STAR: ultrafast universal RNA-seq aligner. *Bioinformatics* , 29(1), pp.15–21.

Dolken, L. et al., 2008. High-resolution gene expression profiling for simultaneous kinetic parameter analysis of RNA synthesis and decay. *RNA* , 14(9), pp.1959–1972.

Dominguez, D. et al., 2017. Sequence, Structure and Context Preferences of Human RNA Binding Proteins. Available at: http://dx.doi.org/10.1101/201996.

Dunning, M.J. et al., 2007. beadarray: R classes and methods for Illumina bead-based data. *Bioinformatics* , 23(16), pp.2183–2184.

Ebert, M.S., Neilson, J.R. & Sharp, P.A., 2007. MicroRNA sponges: competitive inhibitors of small RNAs in mammalian cells. *Nature methods*, 4(9), pp.721–726.

Eichhorn, S.W. et al., 2014. mRNA destabilization is the dominant effect of mammalian microRNAs by the time substantial repression ensues. *Molecular cell*, 56(1), pp.104–115.

Elkon, R., Ugalde, A.P. & Agami, R., 2013. Alternative cleavage and polyadenylation: extent, regulation and function. *Nature reviews. Genetics*, 14(7), pp.496–506.

Ernoult-Lange, M. et al., 2012. Multiple binding of repressed mRNAs by the P-body protein Rck/p54. *RNA* , 18(9), pp.1702–1715.

Fabian, M.R. & Sonenberg, N., 2012. The mechanics of miRNA-mediated gene silencing: a look under the hood of miRISC. *Nature structural & molecular biology*, 19(6), pp.586–593.

Freimer, J.W. et al., 2018. Expression of Alternative Ago2 Isoform Associated with Loss of microRNA-Driven Translational Repression in Mouse Oocytes. *Current biology: CB*, 28(2), pp.296–302.e3.

Friedman, R.C. et al., 2008. Most mammalian mRNAs are conserved targets of microRNAs. *Genome research*, 19(1), pp.92–105.

Fukao, A. et al., 2014. MicroRNAs trigger dissociation of eIF4AI and eIF4AII from target mRNAs in humans. *Molecular cell*, 56(1), pp.79–89.

Fukaya, T., Iwakawa, H.-O. & Tomari, Y., 2014. MicroRNAs block assembly of eIF4F translation initiation complex in Drosophila. *Molecular cell*, 56(1), pp.67–78.

Gambardella, G. et al., 2017. The impact of microRNAs on transcriptional heterogeneity and gene co-expression across single embryonic stem cells. *Nature communications*, 8, p.14126.

Gerstberger, S., Hafner, M. & Tuschl, T., 2014. A census of human RNA-binding proteins.

Nature reviews. Genetics, 15(12), pp.829–845.

Gingold, H. et al., 2014. A dual program for translation regulation in cellular proliferation and differentiation. *Cell*, 158(6), pp.1281–1292.

Giraldez, A.J., 2010. microRNAs, the cell's Nepenthe: clearing the past during the maternal-to-zygotic transition and cellular reprogramming. *Current opinion in genetics & development*, 20(4), pp.369–375.

Glisovic, T. et al., 2008. RNA-binding proteins and post-transcriptional gene regulation. *FEBS letters*, 582(14), pp.1977–1986.

Golden, R.J. et al., 2017. An Argonaute phosphorylation cycle promotes microRNA-mediated silencing. *Nature*, 542(7640), pp.197–202.

Goodarzi, H. et al., 2016. Modulated Expression of Specific tRNAs Drives Gene Expression and Cancer Progression. *Cell*, 165(6), pp.1416–1427.

Greve, T.S., Judson, R.L. & Blelloch, R., 2013. microRNA control of mouse and human pluripotent stem cell behavior. *Annual review of cell and developmental biology*, 29, pp.213–239.

Guan, C. et al., 2010. A review of current large-scale mouse knockout efforts. *Genesis* , 48(2), pp.73–85.

Gu, K.-L. et al., 2016. Pluripotency-associated miR-290/302 family of microRNAs promote the dismantling of naive pluripotency. *Cell research*, 26(3), pp.350–366.

Guo, H. et al., 2010. Mammalian microRNAs predominantly act to decrease target mRNA levels. *Nature*, 466(7308), pp.835–840.

Gu, S. et al., 2012. Slicing-independent RISC activation requires the argonaute PAZ domain. *Current biology: CB*, 22(16), pp.1536–1542.

Hao, S. & Baltimore, D., 2009. The stability of mRNA influences the temporal order of the induction of genes encoding inflammatory molecules. *Nature immunology*, 10(3), pp.281–288.

He, M. et al., 2012. Cell-type-based analysis of microRNA profiles in the mouse brain. *Neuron*, 73(1), pp.35–48.

Heyer, E.E. & Moore, M.J., 2016. Redefining the Translational Status of 80S Monosomes. *Cell*, 164(4), pp.757–769.

Hinnebusch, A.G., 2014. The Scanning Mechanism of Eukaryotic Translation Initiation. *Annual review of biochemistry*, 83(1), pp.779–812.

Hinnebusch, A.G. & Lorsch, J.R., 2012. The mechanism of eukaryotic translation initiation: new insights and challenges. *Cold Spring Harbor perspectives in biology*, 4(10). Available at: http://dx.doi.org/10.1101/cshperspect.a011544.

Hinnebusch, A.G. & Natarajan, K., 2002. Gcn4p, a master regulator of gene expression, is controlled at multiple levels by diverse signals of starvation and stress. *Eukaryotic cell*, 1(1), pp.22–32.

Houbaviy, H.B., Murray, M.F. & Sharp, P.A., 2003. Embryonic Stem Cell-Specific MicroRNAs. *Developmental cell*, 5(2), pp.351–358.

Hubstenberger, A. et al., 2017. P-Body Purification Reveals the Condensation of Repressed mRNA Regulons. *Molecular cell*, 68(1), pp.144–157.e5.

Huch, S. & Nissan, T., 2014. Interrelations between translation and general mRNA degradation in yeast. *Wiley interdisciplinary reviews. RNA*, 5(6), pp.747–763.

Ingolia, N.T., Lareau, L.F. & Weissman, J.S., 2011. Ribosome profiling of mouse embryonic stem cells reveals the complexity and dynamics of mammalian proteomes. *Cell*, 147(4), pp.789–802.

Iwakawa, H.-O. & Tomari, Y., 2015. The Functions of MicroRNAs: mRNA Decay and Translational Repression. *Trends in cell biology*, 25(11), pp.651–665.

Jackson, R.J., Hellen, C.U.T. & Pestova, T.V., 2010. The mechanism of eukaryotic translation initiation and principles of its regulation. *Nature reviews. Molecular cell biology*, 11(2), pp.113–127.

Jonas, S. & Izaurralde, E., 2015. Towards a molecular understanding of microRNA-mediated gene silencing. *Nature reviews. Genetics*, 16(7), pp.421–433.

Jovanovic, M. et al., 2015. Immunogenetics. Dynamic profiling of the protein life cycle in response to pathogens. *Science*, 347(6226), p.1259038.

Kamenska, A. et al., 2014. Human 4E-T represses translation of bound mRNAs and enhances microRNA-mediated silencing. *Nucleic acids research*, 42(5), pp.3298–3313.

Kamenska, A. et al., 2016. The DDX6-4E-T interaction mediates translational repression and P-body assembly. *Nucleic acids research*, 44(13), pp.6318–6334.

Kaneda, M. et al., 2009. Essential role for Argonaute2 protein in mouse oogenesis. *Epigenetics & chromatin*, 2(1), p.9.

Kedde, M. et al., 2010. A Pumilio-induced RNA structure switch in p27-3' UTR controls miR-221 and miR-222 accessibility. *Nature cell biology*, 12(10), pp.1014–1020.

Kedde, M. et al., 2007. RNA-binding protein Dnd1 inhibits microRNA access to target mRNA. *Cell*, 131(7), pp.1273–1286.

Kojima, Y., Tam, O.H. & Tam, P.P.L., 2014. Timing of developmental events in the early mouse embryo. *Seminars in cell & developmental biology*, 34, pp.65–75.

Kozomara, A. & Griffiths-Jones, S., 2014. miRBase: annotating high confidence microRNAs using deep sequencing data. *Nucleic acids research*, 42(Database issue), pp.D68–73.

Krishnakumar, R. et al., 2016. FOXD3 Regulates Pluripotent Stem Cell Potential by Simultaneously Initiating and Repressing Enhancer Activity. *Cell stem cell*, 18(1), pp.104–117.

Krol, J., Loedige, I. & Filipowicz, W., 2010. The widespread regulation of microRNA biogenesis, function and decay. *Nature reviews. Genetics*, 11(9), pp.597–610.

Kuzuoğlu-Öztürk, D. et al., 2016. miRISC and the CCR4-NOT complex silence mRNA targets independently of 43S ribosomal scanning. *The EMBO journal*, 35(11), pp.1186–1203.

Kwon, S.C. et al., 2013. The RNA-binding protein repertoire of embryonic stem cells. *Nature structural & molecular biology*, 20(9), pp.1122–1130.

Lambert, N. et al., 2014. RNA Bind-n-Seq: quantitative assessment of the sequence and structural binding specificity of RNA binding proteins. *Molecular cell*, 54(5), pp.887–900.

Lee, F.C.Y. & Ule, J., 2018. Advances in CLIP Technologies for Studies of Protein-RNA Interactions. *Molecular cell*, 69(3), pp.354–369.

Lei, L. & Spradling, A.C., 2013. Female mice lack adult germ-line stem cells but sustain oogenesis using stable primordial follicles. *Proceedings of the National Academy of Sciences of the United States of America*, 110(21), pp.8585–8590.

Liao, Y., Smyth, G.K. & Shi, W., 2014. featureCounts: an efficient general purpose program for assigning sequence reads to genomic features. *Bioinformatics* , 30(7), pp.923–930.

Liu, J. et al., 2004. Argonaute2 is the catalytic engine of mammalian RNAi. *Science*, 305(5689), pp.1437–1441.

Liu, J. et al., 2005. MicroRNA-dependent localization of targeted mRNAs to mammalian P-bodies. *Nature cell biology*, 7(7), pp.719–723.

Liu, Y., Beyer, A. & Aebersold, R., 2016. On the Dependency of Cellular Protein Levels on mRNA Abundance. *Cell*, 165(3), pp.535–550.

Lugowski, A., Nicholson, B. & Rissland, O.S., 2017. Determining mRNA half-lives on a transcriptome-wide scale. *Methods* . Available at: http://dx.doi.org/10.1016/j.ymeth.2017.12.006.

Lu, R. et al., 2009. Systems-level dynamic analyses of fate change in murine embryonic stem cells. *Nature*, 462(7271), pp.358–362.

Ma, J. et al., 2013. Maternally recruited DCP1A and DCP2 contribute to messenger RNA degradation during oocyte maturation and genome activation in mouse. *Biology of reproduction*, 88(1), p.11.

Ma, J. et al., 2010. MicroRNA activity is suppressed in mouse oocytes. *Current biology: CB*, 20(3), pp.265–270.

Ma, J., Fukuda, Y. & Schultz, R.M., 2015. Mobilization of Dormant Cnot7 mRNA Promotes Deadenylation of Maternal Transcripts During Mouse Oocyte Maturation. *Biology of*

reproduction, 93(2), p.48.

Marson, A. et al., 2008. Connecting microRNA genes to the core transcriptional regulatory circuitry of embryonic stem cells. *Cell*, 134(3), pp.521–533.

Martinez, N.J. & Gregory, R.I., 2013. Argonaute2 expression is post-transcriptionally coupled to microRNA abundance. *RNA* , 19(5), pp.605–612.

Mathys, H. et al., 2014. Structural and biochemical insights to the role of the CCR4-NOT complex and DDX6 ATPase in microRNA repression. *Molecular cell*, 54(5), pp.751–765.

Mayr, C., 2017. Regulation by 3′-Untranslated Regions. *Annual review of genetics*, 51(1), pp.171–194.

Mayr, C. & Bartel, D.P., 2009. Widespread shortening of 3'UTRs by alternative cleavage and polyadenylation activates oncogenes in cancer cells. *Cell*, 138(4), pp.673–684.

Melton, C., Judson, R.L. & Blelloch, R., 2010. Opposing microRNA families regulate self-renewal in mouse embryonic stem cells. *Nature*, 463(7281), pp.621–626.

Minshall, N. et al., 2009. Role of p54 RNA helicase activity and its C-terminal domain in translational repression, P-body localization and assembly. *Molecular biology of the cell*, 20(9), pp.2464–2472.

Moretti, F. et al., 2012. PABP and the poly(A) tail augment microRNA repression by facilitated miRISC binding. *Nature structural & molecular biology*, 19(6), pp.603–608.

Morita, S. et al., 2007. One Argonaute family member, Eif2c2 (Ago2), is essential for development and appears not to be involved in DNA methylation. *Genomics*, 89(6), pp.687–696.

Murchison, E.P. et al., 2007. Critical roles for Dicer in the female germline. *Genes & development*, 21(6), pp.682–693.

Murry, C.E. & Keller, G., 2008. Differentiation of embryonic stem cells to clinically relevant populations: lessons from embryonic development. *Cell*, 132(4), pp.661–680.

Nagarajan, V.K. et al., 2013. XRN 5′→3′ exoribonucleases: Structure, mechanisms and functions. *Biochimica et Biophysica Acta (BBA) - Gene Regulatory Mechanisms*, 1829(6-7), pp.590–603.

Ng, H.-H. & Azim Surani, M., 2011. The transcriptional and signalling networks of pluripotency. *Nature cell biology*, 13(5), pp.490–496.

Nichols, J. & Smith, A., 2010. The origin and identity of embryonic stem cells. *Development* , 138(1), pp.3–8.

Nishihara, T. et al., 2013. miRISC recruits decapping factors to miRNA targets to enhance their degradation. *Nucleic acids research*, 41(18), pp.8692–8705.

Nissan, T. et al., 2010. Decapping activators in Saccharomyces cerevisiae act by multiple

mechanisms. *Molecular cell*, 39(5), pp.773–783.

Ozgur, S. et al., 2015. Structure of a Human 4E-T/DDX6/CNOT1 Complex Reveals the Different Interplay of DDX6-Binding Proteins with the CCR4-NOT Complex. *Cell reports*, 13(4), pp.703–711.

Parchem, R.J. et al., 2014. Two miRNA clusters reveal alternative paths in late-stage reprogramming. *Cell stem cell*, 14(5), pp.617–631.

Parker, R., 2012. RNA Degradation in Saccharomyces cerevisae. *Genetics*, 191(3), pp.671–702.

Pelechano, V., Wei, W. & Steinmetz, L.M., 2015. Widespread Co-translational RNA Decay Reveals Ribosome Dynamics. *Cell*, 161(6), pp.1400–1412.

Pertea, M. et al., 2015. StringTie enables improved reconstruction of a transcriptome from RNA-seq reads. *Nature biotechnology*, 33(3), pp.290–295.

Presnyak, V. et al., 2015. Codon optimality is a major determinant of mRNA stability. *Cell*, 160(6), pp.1111–1124.

Presnyak, V. & Coller, J., 2013. The DHH1/RCKp54 family of helicases: an ancient family of proteins that promote translational silencing. *Biochimica et biophysica acta*, 1829(8), pp.817–823.

Rabani, M. et al., 2011. Metabolic labeling of RNA uncovers principles of RNA production and degradation dynamics in mammalian cells. *Nature biotechnology*, 29(5), pp.436–442.

Racki, W.J. & Richter, J.D., 2006. CPEB controls oocyte growth and follicle development in the mouse. *Development* , 133(22), pp.4527–4537.

Radhakrishnan, A. et al., 2016. The DEAD-Box Protein Dhh1p Couples mRNA Decay and Translation by Monitoring Codon Optimality. *Cell*, 167(1), pp.122–132.e9.

Radhakrishnan, A. & Green, R., 2016. Connections Underlying Translation and mRNA Stability. *Journal of molecular biology*, 428(18), pp.3558–3564.

Rädle, B. et al., 2013. Metabolic Labeling of Newly Transcribed RNA for High Resolution Gene Expression Profiling of RNA Synthesis, Processing and Decay in Cell Culture. *JoVE (Journal of Visualized Experiments)*, (78), pp.e50195–e50195.

Ran, F.A. et al., 2013. Genome engineering using the CRISPR-Cas9 system. *Nature protocols*, 8(11), pp.2281–2308.

Ritchie, M.E. et al., 2015. limma powers differential expression analyses for RNA-sequencing and microarray studies. *Nucleic acids research*, 43(7), p.e47.

Rouya, C. et al., 2014. Human DDX6 effects miRNA-mediated gene silencing via direct binding to CNOT1. *RNA* , 20(9), pp.1398–1409.

Roy, B. & Jacobson, A., 2013. The intimate relationships of mRNA decay and translation.

Trends in genetics: TIG, 29(12), pp.691–699.

Sabi, R. & Tuller, T., 2014. Modelling the efficiency of codon-tRNA interactions based on codon usage bias. *DNA research: an international journal for rapid publication of reports on genes and genomes*, 21(5), pp.511–526.

Sabi, R., Volvovitch Daniel, R. & Tuller, T., 2017. stAIcalc: tRNA adaptation index calculator based on species-specific weights. *Bioinformatics* , 33(4), pp.589–591.

Saitou, M., Kagiwada, S. & Kurimoto, K., 2012. Epigenetic reprogramming in mouse pre-implantation development and primordial germ cells. *Development* , 139(1), pp.15–31.

Sandberg, R. et al., 2008. Proliferating cells express mRNAs with shortened 3' untranslated regions and fewer microRNA target sites. *Science*, 320(5883), pp.1643–1647.

Schwanhäusser, B. et al., 2011. Global quantification of mammalian gene expression control. *Nature*, 473(7347), pp.337–342.

Schwartz, D.C. & Parker, R., 1999. Mutations in translation initiation factors lead to increased rates of deadenylation and decapping of mRNAs in Saccharomyces cerevisiae. *Molecular and cellular biology*, 19(8), pp.5247–5256.

Sharova, L.V. et al., 2009. Database for mRNA Half-Life of 19 977 Genes Obtained by DNA Microarray Analysis of Pluripotent and Differentiating Mouse Embryonic Stem Cells. *DNA research: an international journal for rapid publication of reports on genes and genomes*, 16(1), pp.45–58.

Shenoy, A. & Blelloch, R.H., 2014. Regulation of microRNA function in somatic stem cell proliferation and differentiation. *Nature reviews. Molecular cell biology*, 15(9), pp.565–576.

Shoemaker, C.J. & Green, R., 2012. Translation drives mRNA quality control. *Nature structural & molecular biology*, 19(6), pp.594–601.

Sonenberg, N. & Hinnebusch, A.G., 2009. Regulation of Translation Initiation in Eukaryotes: Mechanisms and Biological Targets. *Cell*, 136(4), pp.731–745.

Song, J.-J. et al., 2004. Crystal structure of Argonaute and its implications for RISC slicer activity. *Science*, 305(5689), pp.1434–1437.

Spies, N., Burge, C.B. & Bartel, D.P., 2013. 3' UTR-isoform choice has limited influence on the stability and translational efficiency of most mRNAs in mouse fibroblasts. *Genome research*, 23(12), pp.2078–2090.

Stein, P. et al., 2015. Essential Role for endogenous siRNAs during meiosis in mouse oocytes. *PLoS genetics*, 11(2), p.e1005013.

Subramanyam, D. et al., 2011. Multiple targets of miR-302 and miR-372 promote reprogramming of human fibroblasts to induced pluripotent stem cells. *Nature biotechnology*, 29(5), pp.443–448.

Subtelny, A.O. et al., 2014. Poly(A)-tail profiling reveals an embryonic switch in translational

control. *Nature*, 508(7494), pp.66–71.

Su, H. et al., 2009. Essential and overlapping functions for mammalian Argonautes in microRNA silencing. *Genes & development*, 23(3), pp.304–317.

Suh, N. et al., 2010. MicroRNA function is globally suppressed in mouse oocytes and early embryos. *Current biology: CB*, 20(3), pp.271–277.

Svoboda, P. & Flemr, M., 2010. The role of miRNAs and endogenous siRNAs in maternal-to-zygotic reprogramming and the establishment of pluripotency. *EMBO reports*, 11(8), pp.590–597.

Svoboda, P., Franke, V. & Schultz, R.M., 2015. Sculpting the Transcriptome During the Oocyte-to-Embryo Transition in Mouse. *Current topics in developmental biology*, 113, pp.305–349.

Sweet, T., Kovalak, C. & Coller, J., 2012. The DEAD-box protein Dhh1 promotes decapping by slowing ribosome movement. *PLoS biology*, 10(6), p.e1001342.

Szostak, E. & Gebauer, F., 2013. Translational control by 3'-UTR-binding proteins. *Briefings in functional genomics*, 12(1), pp.58–65.

Tam, O.H. et al., 2008. Pseudogene-derived small interfering RNAs regulate gene expression in mouse oocytes. *Nature*, 453(7194), pp.534–538.

Tang, F. et al., 2007. Maternal microRNAs are essential for mouse zygotic development. *Genes & development*, 21(6), pp.644–648.

Tritschler, F. et al., 2009. Structural basis for the mutually exclusive anchoring of P body components EDC3 and Tral to the DEAD box protein DDX6/Me31B. *Molecular cell*, 33(5), pp.661–668.

Turner, M. & Díaz-Muñoz, M.D., 2018. RNA-binding proteins control gene expression and cell fate in the immune system. *Nature immunology*, 19(2), pp.120–129.

Van Nostrand, E.L. et al., 2017. A Large-Scale Binding and Functional Map of Human RNA Binding Proteins. *bioRxiv*, p.179648. Available at: https://www.biorxiv.org/content/early/2017/08/23/179648.abstract [Accessed March 10, 2018].

Van Nostrand, E.L. et al., 2016. Robust transcriptome-wide discovery of RNA-binding protein binding sites with enhanced CLIP (eCLIP). *Nature methods*, 13(6), pp.508–514.

de Vries, W.N. et al., 2000. Expression of Cre recombinase in mouse oocytes: a means to study maternal effect genes. *Genesis* , 26(2), pp.110–112.

Wahle, E. & Sebastiaan Winkler, G., 2013. RNA decay machines: Deadenylation by the Ccr4–Not and Pan2–Pan3 complexes. *Biochimica et Biophysica Acta (BBA) - Gene Regulatory Mechanisms*, 1829(6-7), pp.561–570.

Wang, E.S. et al., 2015. Fas-Activated Mitochondrial Apoptosis Culls Stalled Embryonic Stem

Cells to Promote Differentiation. *Current biology: CB*, 25(23), pp.3110–3118.

Wang, Y. et al., 2007. DGCR8 is essential for microRNA biogenesis and silencing of embryonic stem cell self-renewal. *Nature genetics*, 39(3), pp.380–385.

Wang, Y. et al., 2008. Embryonic stem cell-specific microRNAs regulate the G1-S transition and promote rapid proliferation. *Nature genetics*, 40(12), pp.1478–1483.

Watanabe, A., Yamada, Y. & Yamanaka, S., 2013. Epigenetic regulation in pluripotent stem cells: a key to breaking the epigenetic barrier. *Philosophical transactions of the Royal Society of London. Series B, Biological sciences*, 368(1609), p.20120292.

Watanabe, T. et al., 2008. Endogenous siRNAs from naturally formed dsRNAs regulate transcripts in mouse oocytes. *Nature*, 453(7194), pp.539–543.

Windhager, L. et al., 2012. Ultrashort and progressive 4sU-tagging reveals key characteristics of RNA processing at nucleotide resolution. *Genome research*, 22(10), pp.2031–2042.

Xia, Z. et al., 2014. Dynamic analyses of alternative polyadenylation from RNA-seq reveal a 3′-UTR landscape across seven tumour types. *Nature communications*, 5, p.5274.

Ye, J. & Blelloch, R., 2014. Regulation of Pluripotency by RNA Binding Proteins. *Cell stem cell*, 15(3), pp.271–280.

Ying, Q.-L. et al., 2008. The ground state of embryonic stem cell self-renewal. *Nature*, 453(7194), pp.519–523.

Young, R.A., 2011. Control of the Embryonic Stem Cell State. *Cell*, 144(6), pp.940–954.

Zamudio, J.R., Kelly, T.J. & Sharp, P.A., 2014. Argonaute-bound small RNAs from promoter-proximal RNA polymerase II. *Cell*, 156(5), pp.920–934.

Zekri, L., Kuzuoğlu-Öztürk, D. & Izaurralde, E., 2013. GW182 proteins cause PABP dissociation from silenced miRNA targets in the absence of deadenylation. *The EMBO journal*, 32(7), pp.1052–1065.
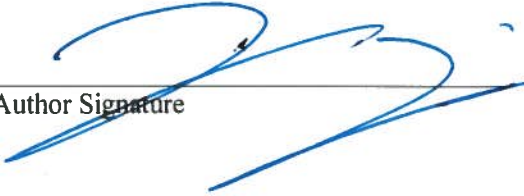
Publishing Agreement

It is the policy of the University to encourage the distribution of all theses, dissertations, and manuscripts. Copies of all UCSF theses, dissertations, and manuscripts will be routed to the library via the Graduate Division. The library will make all theses, dissertations, and manuscripts accessible to the public and will preserve these to the best of their abilities, in perpetuity.

Please sign the following statement:

I hereby grant permission to the Graduate Division of the University of California, San Francisco to release copies of my thesis, dissertation, or manuscript to the Campus Library to provide access and preservation, in whole or in part, in perpetuity.

_____ 3-28-18
Author Signature   Date